

1
2
3
4
5
6
7
8
9
10
11
12
13
14
15
16
17
18
19
20
21
22
23
24

THE YKI-CACTUS (I_KB α)-JNK AXIS PROMOTES TUMOR GROWTH AND PROGRESSION IN DROSOPHILA

Kirti Snigdha¹, Amit Singh^{1, 2, 3, 4}, Madhuri Kango-Singh^{1, 2, 3, 4#}

¹Department of Biology, University of Dayton, Dayton OH 45469; ²Center for Tissue Regeneration and Engineering at Dayton (TREND), University of Dayton, Dayton OH 45469; ³Premedical Programs, University of Dayton, Dayton OH 45469 ⁴Integrative Science and Engineering Center (ISE), University of Dayton, Dayton OH 45469

#Corresponding author: Madhuri Kango-Singh
Phone: 937 229 2531
Email: mkango-singh1@udayton.edu

Running Title: Yorkie-Cactus-Jun Kinase axis in tumor growth

25 **Abstract**

26 Presence of inflammatory factors in the tumor microenvironment is well known yet their specific
27 role in tumorigenesis is elusive. The core inflammatory pathways are conserved in *Drosophila*,
28 including the Toll-Like Receptor (TLR) and the Tumor Necrosis Factor (TNF) pathway. We
29 used *Drosophila* tumor models to study the role of inflammatory factors in tumorigenesis.
30 Specifically, we co-activated oncogenic forms of *Ras*^{V12} or its major effector Yorkie (*Yki*^{3SA}) in
31 polarity deficient cells mutant for tumor suppressor gene *scribble* (*scrib*) marked by GFP under
32 *nubGALA* or in somatic clones. This system recapitulates the clonal origins of cancer, and shows
33 neoplastic growth, invasion and lethality. We investigated if TLR and TNF pathway affect
34 growth of *Yki*^{3SA}*scrib*^{RNAi} or *Ras*^{V12}*scrib*^{RNAi} tumors through activation of tumor promoting Jun N-
35 terminal Kinase (JNK) pathway and its target Matrix Metalloprotease1 (MMP1). We report, TLR
36 component, Cactus (Cact) is highly upregulated in *Yki*^{3SA}*scrib*^{RNAi} or *Ras*^{V12}*scrib*^{RNAi} tumors.
37 *Drosophila* Cactus (mammalian I κ B α) acts as an inhibitor of NF κ B signaling that plays key
38 roles in inflammatory and immune response. Here we show an alternative role for Cactus, and by
39 extension cytokine mediated signaling, in tumorigenesis. Downregulating Cact affects both
40 tumor progression and invasion. Interestingly, downregulating TNF receptors in tumor cells did
41 not affect their invasiveness despite reducing JNK activity. Genetic analysis suggested that Cact
42 and JNK are key regulators of tumor progression. Overall, we show that Yki plays a critical role
43 in tumorigenesis by controlling Cact, which in turn, mediates tumor promoting JNK oncogenic
44 signaling in tumor cells.

45 **Key words:** Cancer, Yki, Ras, Inflammation, Signaling pathway, Proliferation, Invasion

46

47

48 Introduction

49 Oncogenic forms of Ras are dominant drivers of tumor growth in a third of human
50 cancers (1). Oncogenic Ras activates multiple downstream pathways like PI3K, RAF-MEK-
51 MAPK, JNK, p38 MAPK during tumorigenesis (2). *Drosophila* tumor models of oncogenic Ras
52 (*Ras^{V12}*) with *scribble* (*scrib*) – the apical basal polarity regulator (referred as *Ras^{V12}scrib⁻*
53 tumors), show neoplastic growth, invasion and lethality (3, 4). In *Ras^{V12} scrib⁻* tumors, Eiger
54 (Egr), the ligand of *Drosophila* TNF, induces Jun N-terminal Kinase (JNK) pathway to promote
55 tumor cell proliferation (5, 6). In contrast, Egr mediates elimination of defective cells through
56 JNK specifically in *scrib* mosaic clones (7). Inflammatory components from the Toll Like
57 Receptor (TLR) and Tumor Necrosis Factor (TNF) pathways play a significant role in tumor
58 progression through poorly understood mechanisms (8, 9). However, the complex signaling
59 initiated by oncogenic Ras presents challenges to deciphering the role of key inflammatory
60 signals in tumor growth and progression.

61 A key effector of oncogenic Ras signaling is the Hippo pathway transcriptional
62 coactivator protein Yki (*Drosophila* YAP ortholog) (10-12). Furthermore, elevated YAP activity
63 is linked to neoplastic behavior in cancer cells, and poor prognosis in several cancers (13-15). To
64 study the role of these inflammatory pathways in tumorigenesis, we established a Yki dependent
65 model by expressing activated form of Yki (*UASYki^{3SA}*) in cells where *scrib* is downregulated
66 (*UASscrib^{RNAi}*) using the GAL4-UAS system or in ‘flip-out’ clones. *Yki^{3SA}scrib^{RNAi}* tumors show
67 key hallmarks of cancer such as sustained proliferation via JNK activation (pJNK), Matrix
68 Metalloprotease 1 (MMP1) mediated invasion, and degradation of basement membrane due to
69 loss of Laminin. Using these models, we show that the *Drosophila* I κ B α orthologue Cactus
70 (Cact), a member of the TLR pathway (16), is upregulated in both *Yki^{3SA}scrib^{RNAi}* and

71 *Ras*^{VI2}*scrib*^{RNAi} clones. Downregulation of Cact (*UAS-cact*^{RNAi}) in the tumor clones results in
72 downregulation/suppression of pJNK and MMP1. We show that Cact acts upstream of JNK, and
73 JNK activation may occur independent of Wengen (Wgn) and Grindelwald (Grnd), the
74 *Drosophila* TNF Receptors that signal through the JNK pathway (17). Furthermore, we report a
75 novel Yki-Cact-JNK signaling axis that promotes tumorigenesis downstream of Yki activation
76 that is critical in promoting Ras or Yki mediated tumor growth. The Yki-Cact-JNK axis plays a
77 critical role, as downregulation of Yki or Sd (*Drosophila* TEAD family transcription factor), or
78 Cact or JNK disrupts this signaling axis and inhibits *Ras*^{VI2}*scrib*^{RNAi} tumorigenesis.

79 **Results**

80 **Comparison of oncogenic Yki and Ras dependent tumor models**

81 We coexpressed oncogenic Yki (*UASYki*^{3SA}), *scrib*^{RNAi} (*UASscrib*^{RNAi}) and GFP
82 (*UASGFP*) using *nub-Gal4* in wing imaginal discs [*nub>GFPYki*^{3SA}*scrib*^{RNAi}] (**Fig. 1A**)(18).
83 Compared to wild-type [*nub>GFP*], the *Yki*^{3SA}*scrib*^{RNAi} larvae appeared bloated, with overgrown
84 wing discs (**Fig. 1A'**), entered an extended larval life, and were 100% pupal lethal. The dissected
85 wing discs revealed large neoplastic growths confined to the wing pouch (detected by GFP
86 expression) (**Fig. S1A**). These neoplasms were invasive (**Fig. 1B**), as tumor cells (GFP positive)
87 extruded to the basal side and breached the basement membrane labelled with Laminin (red)
88 (**Fig. 1B, B'**)(3, 19). The *nub>Yki*^{3SA}*scrib*^{RNAi} system produced massive multilayered tumors with
89 high lethality, therefore, in parallel we made heat-shock mediated 'Flp-out' clones driven by
90 *Act>y+>Gal4* (20, 21). The wild-type clones detected by co-expression of GFP
91 (*AyGal4>UASGFP*) in the epithelial monolayer showed jagged clone boundaries (**Fig. S1B,**
92 **C**)(22), whereas the *Yki*^{3SA}*scrib*^{RNAi} clones (*AyGal4>UASGFP,UASYki*^{3SA},*UASscrib*^{RNAi})
93 presented as large epithelial outgrowths with well-sorted smooth borders (**Fig. 1C**). Compared to

94 wild-type clones (thickness 11 μ m), the *Yki^{3SA}scrib^{RNAi}* clones are multilayered (23.17 μ m) (**Fig.**
95 **S1C**). Under comparable experimental conditions, the *Ras^{V12}scrib^{RNAi}* larvae (120h AEL) looked
96 thin and sluggish, and dissected imaginal discs were fragile, neoplastic, and comprised
97 exclusively of GFP-positive cells. When the heat shock was reduced to 3min, *Ras^{V12}scrib^{RNAi}*
98 ‘flp-out’ clones also showed multi-layered organization (**Fig. S1C**). JNK mediated pro-
99 proliferative signaling promotes tumorigenesis (8, 23-25). Consistent with this, the JNK reporter
100 *puc^{E69}-lacZ* (26) was induced in *Ras^{V12}scrib^{RNAi}* and *Yki^{3SA}scrib^{RNAi}* clones (**Fig. 1C, D**).
101 Furthermore, pJNK levels are also upregulated in *Ras^{V12}scrib^{RNAi}* and *Yki^{3SA}scrib^{RNAi}* clones (**Fig.**
102 **S1D, E**). Next, to assess invasive capacity we assessed MMP1 expression in our tumor models
103 (27-30). MMP1 expression is very low in wild-type clones (**Fig S1F**), however, MMP1 is
104 robustly induced in both *Yki^{3SA}scrib^{RNAi}* and *Ras^{V12}scrib^{RNAi}* tumor clones (**Fig. 1E, F**).
105 Quantification of the integrated pixel intensity of MMP1 expression in *Yki^{3SA}scrib^{RNAi}* clone
106 showed a 4-fold increase compared to the surrounding normal cells (**Fig. 1G**). Taken together,
107 these data suggest that *nub>Yki^{3SA}scrib^{RNAi}* and *Ay>Yki^{3SA}scrib^{RNAi}* clones recapitulate key
108 tumorigenic features of the well-established *Ras^{V12}scrib^{RNAi}* model like increased proliferation,
109 formation of multilayered invasive neoplasms capable of basement membrane degradation, and
110 induction of JNK signaling. Using these models, we investigated the role of key inflammatory
111 pathways (TLR and TNF) in tumorigenesis.

112 ***Drosophila* I κ B α component, Cactus, is upregulated in the tumor clones**

113 Cact prevents TLR activation by associating with and blocking nuclear localization of
114 Dorsal, the *Drosophila* NF- κ B homologue (Dl) or Dorsal-related Immunity Factor (Dif), two
115 effectors of the TLR pathway (16). First, we evaluated Cact expression in tumor cells (16). Cact
116 is ubiquitously expressed, and Cact levels are not affected in wild-type and *scrib^{RNAi}* clones (**Fig.**

117 **2A, B**, quantified in **Fig. 2E**). However, Yki^{3SA} and $Yki^{3SA} scrib^{RNAi}$ clones showed significant
118 upregulation of Cact expression (**Fig. 2C, D** quantified in **Fig. 2E**). Likewise, both
119 $Ras^{V12} scrib^{RNAi}$ clones (**Fig. S2A**, quantified in **Fig. S2B**), and $nub > Yki^{3SA} scrib^{RNAi}$ tumors in the
120 wing discs (**Fig. S2C**) showed increased Cact expression. Taken together, our data suggests that
121 tumor cells have increased Cact expression compared to surrounding normal cells. To test if Cact
122 is required for tumorigenesis, we expressed $UAS-cact^{RNAi}$ and checked if JNK activity is altered
123 when Cact is downregulated in tumor cells. No significant changes in pJNK expression were
124 seen in wild-type ($AyGal4 > cact^{RNAi}$) (**Fig. 2F**, quantified in **Fig. S2D**) or in $scrib$ mutant clones
125 ($AyGal4 > cact^{RNAi} scrib^{RNAi}$) (**Fig. 2G**, quantified in **Fig. S2D**). Interestingly, downregulation of
126 Cact affected cell sorting but not clone size as the jagged clone boundaries in $scrib^{RNAi}$ clones
127 (**Fig. 2B**), were altered to well-sorted smooth borders in $cact^{RNAi} scrib^{RNAi}$ clones (**Fig. 2G**). In
128 $Yki^{3SA} cact^{RNAi}$ (**Fig. 2H**, quantified in **Fig. S2D**) and $Yki^{3SA} scrib^{RNAi} cact^{RNAi}$ clones (**Fig. 2I**,
129 quantified in **J**), downregulation of $cact$ prevented pJNK induction, and reduced pJNK
130 expression to wild-type levels. Next, we evaluated the invasiveness of tumor clones when $cact$
131 was downregulated. Downregulation of $cact$ in wild-type (**Fig. 2K**) or $scrib^{RNAi}$ (**Fig. 2L**,
132 quantified in **Fig. S2F**) clones did not affect MMP1 expression. In $Yki^{3SA} cact^{RNAi}$ clones MMP1
133 levels were significantly reduced (**Fig. 2M**) when compared to Yki^{3SA} clones, but were
134 significantly higher than wild-type clones (**Fig. S2F, G**). Remarkably, MMP1 levels are reduced
135 to wild-type in $Yki^{3SA} scrib^{RNAi} cact^{RNAi}$ clones (**Fig. 2N**, quantified in **O**) although these clones
136 may still be multi-layered (**Fig. S2E**). Overall, our data showed that decreasing levels of $cact$ in
137 the tumor cells reduced JNK activation and MMP1 induction, thereby affecting tumor growth
138 and invasiveness. Interestingly, $nub > Yki^{3SA} scrib^{RNAi} cact^{RNAi}$ wing discs also showed reduced
139 pJNK (**Fig. S2H**) and MMP1 (**Fig. S2I**) expression when compared to $nub > Yki^{3SA} scrib^{RNAi}$ wing

140 discs. The difference in pJNK and MMP1 reduction can be attributed to inherent differences in
141 tumor induction mechanism *viz.*, by a short pulse of Flippase expression in the ‘flip-out’ clones
142 versus sustained Gal4 driven expression. Overall, these data suggest that elevated levels of *cact*
143 play a key role in tumorigenesis, and downregulation of *cact* affects tumor growth by
144 downregulating JNK signaling.

145 **TNF pathway affects tumor growth but not invasiveness**

146 Upregulation of the *Drosophila* TNF ligand Egr is shown to induce JNK activity in
147 *Ras^{V12}scrib^{RNAi}* tumors (5, 6). Egr requires TNF receptors Wgn and /or Grnd for signaling, and
148 downregulation of *wgn* can attenuate Egr activity (31, 32). Hence to manipulate Egr activity in
149 tumor clones, we first downregulated *wgn* through RNA interference in the *Yki^{3SA}scrib^{RNAi}*. No
150 significant change in pJNK(**Fig. 3A**, quantified in **E**) or MMP1 (**Fig. 3F**, quantified in **J**)
151 expression was observed in clones expressing *wgn^{RNAi}*, or *scrib^{RNAi}wgn^{RNAi}* (**Fig. 3B, G**).
152 However, the size of *scrib^{RNAi}wgn^{RNAi}* clones was significantly smaller than *scrib^{RNAi}* clones (**Fig.**
153 **S3A**). This is consistent with previous reports where *scrib,egr* double mutant clones grew poorly
154 compared to *scrib* mutant clones (7). In *Yki^{3SA}wgn^{RNAi}* clones pJNK upregulation is blocked (**Fig.**
155 **3C**, quantified in **Fig. S3B**). However, compared to *Yki^{3SA}* clones, MMP1 was robustly induced
156 in *Yki^{3SA}wgn^{RNAi}* clones (**Fig. 3H**, quantified in **Fig. S3C, D**). Similarly, in *Yki^{3SA}scrib^{RNAi}wgn^{RNAi}*
157 clones pJNK activation is suppressed (**Fig. 3D**, quantified in **E**). Interestingly, MMP1 is
158 significantly upregulated in *Yki^{3SA}scrib^{RNAi}wgn^{RNAi}* clones comparable to levels in *Yki^{3SA}scrib^{RNAi}*
159 clones (**Fig. 3I**, quantified in **Fig. 3J**). Similar findings were reported in *Ras^{V12}scrib^{RNAi}wgn^{RNAi}*
160 tumors or chromosomal instability induced tumor models where MMP1 induction is not affected
161 by downregulation of *wgn* (17, 33). These data suggested that either the wild-type levels of

162 pJNK are sufficient for MMP1 induction in tumors, or Grnd, the other TNF receptor, regulates
163 the activation of TNF-JNK pathway during tumor growth and invasion.

164 We could not generate *Act>y+>Gal4UASgrnd^{RNAi}* recombined lines since ‘flp-out’
165 clones made with *eyFLP* or *hsFLP* lacked a definitive phenotype. However, we succeeded in
166 recombining *nubGal4 UASGFP* with *UASgrnd^{RNAi}* flies (details in supplementary methods).
167 Similar to *wgn^{RNAi}*, pJNK levels were significantly reduced in wing discs from
168 *Yki^{3SA}scrib^{RNAi}grnd^{RNAi}* larvae when compared to *Yki^{3SA}scrib^{RNAi}*, but significantly higher than
169 wild-type (*nub>GFP*) levels (**Fig. S4A**, quantified in **Fig. 3K**). However, MMP1 was still
170 significantly induced (**Fig. S4B** quantified in **Fig. 3L**). Previous reports show that tumors caused
171 by chromosomal instability show high MMP1 induction despite *grnd* downregulation (33). To
172 account for the possible functional redundancy between Wgn and Grnd, we downregulated both
173 receptors and evaluated MMP1 expression in *Yki^{3SA}scrib^{RNAi}* tumors. Compared to
174 *nub>Yki^{3SA}scrib^{RNAi}*, downregulation of both TNF receptors
175 (*nub>Yki^{3SA}scrib^{RNAi}grnd^{RNAi}wgn^{RNAi}*) reduced pJNK levels significantly (**Fig. S4C**, quantified
176 in **Fig. 3K**), but no significant reduction in MMP1 expression was observed (**Fig. S4D**,
177 quantified in **Fig. 3L**). Taken together, these data suggest that tumor growth but not invasiveness
178 is regulated by TNF pathway receptors.

179 **JNK regulates invasiveness but not Cact expression in the tumor**

180 Although downregulating TNF receptors didn’t affect MMP1 induction in the tumor cells
181 (**Fig. 3K, L**), downregulating TLR component, Cact, reduced MMP1 expression to wild-type
182 levels (**Fig. 2O**). Given that JNK is the key MAPK that can transcriptionally activate MMP1(27),
183 we investigated if Cact can intracellularly activate JNK independent of the TNF receptors and
184 cause MMP1 activation in tumor cells. We compared pJNK and MMP1 expression in the

185 *Yki*^{3SA}*scrib*^{RNAi} *wgn*^{RNAi} clones when JNK activity was inhibited by expressing dominant negative
186 form of *Drosophila* JNK, *bsk*^{DN} (34). As expected, downregulation of JNK in the *Yki*^{3SA} *scrib*^{RNAi}
187 clones (*Yki*^{3SA}*scrib*^{RNAi}*bsk*^{DN}) inhibited both pJNK activation (**Fig. 4A**, quantified in **D**) and
188 MMP1 induction (**Fig. 4E**, quantified in **G**). Interestingly, co-expression of *bsk*^{DN} with
189 *Yki*^{3SA}*scrib*^{RNAi}*wgn*^{RNAi}, blocked both pJNK (**Fig. 4B**, quantified in **D**) and MMP1 induction (**Fig.**
190 **4F** quantified in **G**). Thus, in tumor cells MMP1 expression can be stimulated by a TNF
191 receptor-independent intracellular JNK activation mechanism. Furthermore, downregulation of
192 JNK and *Wgn* significantly reduced clone thickness (15.63µm) (**Fig. 4C**) as compared to that of
193 *Yki*^{3SA}*scrib*^{RNAi} tumors (23.17µm). Interestingly while *Cact* downregulation affected JNK
194 activation, downregulating JNK in tumor clones (*bsk*^{DN}*Yki*^{3SA}*scrib*^{RNAi}) showed significant *Cact*
195 expression similar to *Yki*^{3SA}*scrib*^{RNAi} tumor clones (**Fig. 4H**, quantified in **I**). Thus our data
196 showed, *Cact* acts upstream of JNK signaling, and affects oncogenic JNK signaling.

197 **Yki regulates Cact and JNK in promoting tumor survival and invasiveness**

198 Oncogenic cooperation can induce Yki and JNK activity in a context-dependent manner
199 (35, 36), and during anti-microbial response Yki can transcriptionally regulate *Cact* expression
200 (37). Given this, we investigated the role of Yki in regulating *Cact* and JNK levels in our tumor
201 models. We downregulated the levels of Yki (*UASyki*^{RNAi}) in *Ras*^{V12}*scrib*^{RNAi} tumor clones. Under
202 our experimental condition (5min heat shock at 37°C to second instar larvae), clones expressing
203 *yki*^{RNAi} were competed out when the larvae were grown at 25°C or 18°C. Therefore, to prevent
204 elimination of *yki*^{RNAi} clones, we co-expressed *p35*- a pan caspase inhibitor for our experiments
205 (38). Co-expression of *p35* and *yki*^{RNAi} didn't affect *Cact* expression in the wild-type (**Fig. 5A**),
206 *scrib*^{RNAi} (**Fig. 5B**), or *Ras*^{V12} clones (**Fig. 5C**). In comparison to control clones (**Fig. 5A-C**), the
207 *Ras*^{V12}*scrib*^{RNAi}*yki*^{RNAi} clones survived, but showed significant reduction in both the clone size

208 (Fig. 5E) and thickness (Fig. 5F). Interestingly, in *Ras^{V12}scrib^{RNAi}yki^{RNAi}* clones downregulation
209 of Yki blocked Cact (Fig. 5D, quantified in G), pJNK (Fig. S5A) and MMP1 (Fig. S5B)
210 induction as compared to *Ras^{V12}scrib^{RNAi}* clones.

211 The TEAD family transcription factor Scalloped (Sd) is the major binding partner for Yki
212 mediated transcription (39-41). The Yki/Sd complex also regulates *cact* expression during innate
213 immune response (37). Sd downregulation (*nub>sd^{RNAi}*) resulted in a diminished wing pouch
214 and yielded adult flies with smaller wings (42). Cact levels are not affected in wing discs from
215 *nub>sd^{RNAi}* (Fig. 5H) or *nub>scrib^{RNAi}sd^{RNAi}* larvae (Fig. 5I). High larval lethality was seen in
216 *nub>Ras^{V12}sd^{RNAi}* and *nub>Ras^{V12}scrib^{RNAi}sd^{RNAi}* larvae grown at 25°C. However, at 18°C, Cact
217 was not induced in *Ras^{V12}sd^{RNAi}* (Fig. 5J) and *Ras^{V12}scrib^{RNAi}sd^{RNAi}* wing discs (Fig. 5K,
218 quantified in L). In addition, pJNK and MMP1 expression were also not induced in
219 *Ras^{V12}scrib^{RNAi}sd^{RNAi}* wing pouch (Fig. S5C, D). These results strongly support a model where
220 Yki and Sd regulate Cact expression, and loss of either Yki or Sd is sufficient to prevent the
221 upregulation of Cact in the tumor cells. Further downregulation of Yki, Sd or Cact is sufficient to
222 cause downregulation of JNK-mediated sustained signaling that promotes proliferation and
223 invasion. These results suggest a mechanism in which polarity deficient cells with activated Ras
224 require Yki mediated Cact induction and JNK activation to drive tumor growth and invasiveness
225 (Fig. 6).

226 Discussion

227 Yki dependent signals downstream of Oncogenic Ras promote tumor growth

228 Oncogenic Ras activation results in burst of signaling through downstream effectors (Raf, Rac,
229 Rho, PI3K), which phosphorylate and activate transcription factors, such as c-Myc, c-Jun, and c-

230 Fos (27, 43). The plethora of downstream signals make it difficult to identify and analyze key
231 signaling nodes that promote tumor growth. Recently, Hippo pathway effectors YAP/Yki have
232 emerged as key effectors of activated Ras signaling (11, 12, 14, 15). Moreover, YAP/Yki are
233 sites of signal convergence and integration in many mammalian cancers e.g., colon, pancreatic
234 and lung cancer (13, 44). The JNK pathway has emerged as another tumor promoting mechanism
235 that can exert both anti- and pro-tumor activities (24, 45). JNK signaling induces Yki activation
236 during compensatory cell proliferation and neoplastic tumor growth (7, 36, 46, 47), and JNK
237 suppresses Yki elevation in *scrib* mutant cells during growth regulation (48, 49). Thus, JNK,
238 Yki, and their downstream transcription factors have emerged as synergistic drivers of tumor
239 growth (35, 50-53).

240 Consistent with previous reports, overexpression of *Yki*^{3SA} alone leads to hyperplasia, and
241 homozygous loss of *scrib* induces neoplasia (42, 54, 55). When *Yki*^{3SA}*scrib*^{RNAi} are co-expressed,
242 multilayered metastatic tumors formed that degrade the basement membrane (**Fig. 1**). We
243 confirmed that JNK signaling is activated in *Yki*^{3SA}*scrib*⁻ induced neoplastic growth (**Fig. 1**).
244 Polyploid giant cells in *Ras*^{V12}*scrib*^{-/-} clones are linked to increased Yki and JNK activity that
245 promotes tumor progression (56). Variation in cell size is usually seen in primary tumor cells
246 whereas larger metastases show more uniform size (57). We found cells of variable size in the
247 *Yki*^{3SA}*scrib*^{RNAi} clones (**Fig.1C**) but uniform sized in *nub*>*Yki*^{3SA}*scrib*^{RNAi} discs. Further, impaired
248 Hippo signaling can induce JNK signaling via transcriptional activation of the Rho1-GTPase
249 which mediates Yki-induced JNK activation and overgrowth (58). Similarly, in mammals,
250 GPCRs can activate YAP/TAZ through RhoA suggesting Yki-Rho1-JNK axis involvement in
251 bridging the two pathways (58, 59). Our data and other published work suggests that both Yki
252 and JNK dependent signaling is activated in multiple tumor contexts including *Yki*^{3SA}*scrib*^{RNAi}

253 tumors. A key transcriptional target of JNK signaling is MMP1- a matrix metalloprotease
254 required for tissue remodeling, wound healing, regeneration, and control of cell movement and
255 cell adhesion during development; and degradation of the basement membrane during tumor
256 invasion (25, 27-29, 60, 61). We used JNK activation and MMP1 induction as the criteria to
257 evaluate tumor growth and invasiveness. The *Yki^{3SA}scrib^{RNAi}* tumor clones showed high levels of
258 JNK activity and MMP1 induction (**Fig. 1**) suggesting that the tumor cells have acquired
259 invasive traits.

260 **Yki regulates Cact and JNK in Tumor cells**

261 Cact is a negative regulator of the *Drosophila* Rel/NFκB orthologues Dorsal, Dif and
262 Relish. Degradation of Cact, allows NFκB activation and localization to nucleus where it
263 regulates transcription of genes controlling inflammatory cytokines and cell growth (62, 63).
264 However, we noticed an accumulation of Cact in our tumor clones. (**Fig. 2**). Downregulating
265 Cact in tumor cells prevented tumor progression by suppressing JNK activation and MMP1
266 induction (**Fig. 2**). This indicated a role of Cact in promoting tumor progression. Increase in Toll
267 signaling by downregulation of Cact aggravates JNK activated cell death (64). Interestingly, we
268 observed a significant reduction in pJNK expression with downregulation of Cact in our tumor
269 clones (**Fig. 2**). These observations indicate that IκBα can regulate proliferation through JNK.
270 Moreover, we found that downregulating JNK by downregulating TNF receptors (**Fig. 3**) did not
271 affect MMP1 induction in our tumor clone. Also, downregulation of JNK by expressing
272 dominant negative form of JNK (**Fig. 4**), did not affect Cact expression in the tumor cells
273 although it blocked JNK and MMP1 activation (**Fig. 4**). Based on these genetic interactions, we
274 concluded that Cact acts upstream of JNK and plays a key role in regulation of oncogenic JNK
275 signaling (**Fig. 6**). We also observed that Wgn downregulation in tumor clones did not affect

276 Cact accumulation (data not shown). Although JNK levels were reduced, MMP1 was still
277 induced in such cells (**Fig. 3**). Since TNFR1 can antagonistically regulate cell cycle through JNK
278 and NFκB (65), it will be interesting to explore whether such signaling crosstalk between these
279 three pathways affects mammalian tumorigenesis.

280 JNK is known to play a context dependent role to promote tumor growth. Work from our
281 lab and others found that, Yki can also regulate JNK activation in the tumor cells. Liu et al.
282 demonstrated that Yki can regulate the TLR pathway and prevent antimicrobial response (37).
283 They showed that in the *Drosophila* larval fat body, Yki along with its transcriptional co-
284 activator Scalloped, is capable of activating Cact. We also observed that downregulating either
285 Yki or Scalloped severely affected tumor growth and showed no overexpression of Cact (**Fig. 5**).
286 Further, downregulating Yki in tumor cells also restored JNK level. Similarly, in Basal Cell
287 Carcinoma YAP interacts with its DNA binding transcription factors, TEAD and promotes c-Jun
288 activity while loss of YAP leads to reduction in phosphorylated JNK and JUN (66). Overall,
289 based on these data we propose a new mechanism where Yki functions with Sd to activate Cact
290 and regulate JNK induction in the tumor cells (**Fig. 6**). Although *cact* is a transcriptional target of
291 the Yki/Sd complex during innate immune response (37), whether this interaction is involved in
292 tumor immunogenicity remains unknown. Recent studies have shown that inactivation of Hippo
293 pathway in tumor cells induces host inflammatory responses, and the pathway can respond to
294 and mediate inflammatory signals (67, 68). In conclusion, our study unraveled the interaction
295 between the Yki, JNK and Cact to drive tumorigenesis. Therefore, it will be interesting to
296 explore the mechanisms underlying the role of innate immunity in tumor progression and
297 metastasis.

298 **Material and methods**

299 **Fly Strains and Generation of Clones:** All fly mutant and transgenic lines are described in
300 Flybase, and were obtained from the Bloomington Drosophila Stock Center unless otherwise
301 specified. *UAS-GFP* labeled clones were produced in larval imaginal discs using the following
302 strains: *nub-Gal4/CyO* (from S. Cohen), *yw; Act>y+>Gal4,UAS-GFP* (BL4411),
303 *UASYki^{3SA}*(BL28817), *UASscrib^{RNAi}* (BL58085, BL59080), *UASwgn^{RNAi}* (BL50594),
304 *UASgrnd^{RNAi}/CyO* (from A. Bergmann), *UAScact^{RNAi}* (BL31713), *UASRas^{V12}* (BL5788),
305 *UASbsk^{DN}* (BL6409), *UASyki^{RNAi}* (BL34067), *UASsd^{RNAi}*(BL29352),*UASP35*, and *puc^{E69}-lacZ*.
306 Appropriate genetic crosses were performed to establish recombined fly stocks to generate
307 clones of the indicated genotypes. To induce somatic clones, larvae (48 hr after egg laying) were
308 heat shocked at 37°C for 5 min. This heat shock regimen was followed to induce *Yki^{3SA} scrib^{RNAi}*
309 clones alone or in combination with other transgenes described in the manuscript.

310 **Immunohistochemistry:** Third instar larvae were dissected and processed for
311 immunohistochemistry following standard protocol (69).The samples were mounted in the
312 VectaShield mounting medium (Vector Labs) and scanned using confocal microscopy (Olympus
313 Fluoview 1000, 3000). The primary antibodies used were mouse anti-Cact (DHSB, 1:200), rabbit
314 anti-pJNK (Cell Signaling Technology, 1:250), mouse anti-β gal (DSHB, 1:250), rabbit anti-
315 Laminin (Ab-Cam,1:250) and mouse anti-MMP1 (DHSB, 1:200). Secondary antibody used
316 were donkey Cy3-conjugated anti-mouse IgG (1:200, Jackson ImmunoResearch), and donkey
317 Cy3-conjugated anti-rabbit IgG (1:200, Jackson ImmunoResearch).

318 **Quantification:** The immunohistochemistry data was quantified using the measurement log
319 function of Photoshop (Adobe Photoshop CC 2018). For the heat shock induced clones, 3
320 circular ROI of 50pixel radius were used per clone (GFP positive) and adjacent normal region
321 (GFP-negative). For the *nubGAL4* driven experiments, 3 square ROIs of 100 pixel length were

322 used. The average value of the integrated density was compared in between the normal non-GFP
323 and clone specific GFP positive cells. For comparison between two different genotypes, ratio of
324 the average integrated density in the GFP positive and negative region was compared. A ratio of
325 1 indicated no change in expression level between the tumor (GFP positive) and normal (GFP
326 negative) region. In all studies, the change in expression compared between different genotypes
327 is normalized with wild-type levels set to 1. Thickness of the clones was measured using the
328 inbuilt ruler of the Fluoview 3000 software in the XZ/YZ optical sections for all experiments.
329 Statistical significance was quantified by Student t-test using Graphpad Prism 5 software.

330

331 **Acknowledgements**

332 We would like to thank, Dr. A. Bergmann, Dr. Stephen Cohen, the Bloomington Drosophila
333 Stock Center, and the Drosophila Studies Hybridoma Bank for flies and antibodies. KS
334 acknowledge the Teaching Assistantship and Graduate Student Summer Fellowship (GSSF)
335 from the Graduate Program of University of Dayton. AS is supported by Start-up research funds
336 and funding from Schuellein Endowed Chair in Biology from the University of Dayton and NIH
337 1R15 GM124654-1. MKS is supported by start-up research funds from the University of Dayton,
338 and a subaward from NIH grant R01CA183991 (PI Nakano).

339

340 **Conflict of Interest**

341 The authors declare no conflict of interest.

342 **Supplementary information is available at Oncogene's website.**

343 **References**

- 344 1. Fernandez-Medarde A, Santos E. Ras in cancer and developmental diseases. *Genes*
345 *Cancer*. 2011;2(3):344-58.
- 346 2. Young A, Lou D, McCormick F. Oncogenic and wild-type Ras play divergent roles in the
347 regulation of mitogen-activated protein kinase signaling. *Cancer Discov*. 2013;3(1):112-23.
- 348 3. Pagliarini RA, Xu T. A genetic screen in *Drosophila* for metastatic behavior. *Science*.
349 2003;302(5648):1227-31.
- 350 4. Brumby AM, Richardson HE. scribble mutants cooperate with oncogenic Ras or Notch to
351 cause neoplastic overgrowth in *Drosophila*. *EMBO J*. 2003;22(21):5769-79.
- 352 5. Cordero JB, Macagno JP, Stefanatos RK, Strathdee KE, Cagan RL, Vidal M. Oncogenic
353 Ras diverts a host TNF tumor suppressor activity into tumor promoter. *Dev Cell*.
354 2010;18(6):999-1011.
- 355 6. Igaki T, Kanda H, Yamamoto-Goto Y, Kanuka H, Kuranaga E, Aigaki T, et al. Eiger, a
356 TNF superfamily ligand that triggers the *Drosophila* JNK pathway. *EMBO J*. 2002;21(12):3009-
357 18.
- 358 7. Ohsawa S, Sugimura K, Takino K, Xu T, Miyawaki A, Igaki T. Elimination of oncogenic
359 neighbors by JNK-mediated engulfment in *Drosophila*. *Dev Cell*. 2011;20(3):315-28.
- 360 8. Hanahan D, Weinberg RA. Hallmarks of cancer: the next generation. *Cell*.
361 2011;144(5):646-74.
- 362 9. Mantovani A, Allavena P, Sica A, Balkwill F. Cancer-related inflammation. *Nature*.
363 2008;454(7203):436-44.
- 364 10. Shao DD, Xue W, Krall EB, Bhutkar A, Piccioni F, Wang X, et al. KRAS and YAP1
365 converge to regulate EMT and tumor survival. *Cell*. 2014;158(1):171-84.
- 366 11. Kapoor A, Yao W, Ying H, Hua S, Liewen A, Wang Q, et al. Yap1 activation enables
367 bypass of oncogenic Kras addiction in pancreatic cancer. *Cell*. 2014;158(1):185-97.
- 368 12. Snigdha K, Gangwani KS, Lapalnikar GV, Singh A, Kango-Singh M. Hippo Signaling in
369 Cancer: Lessons From *Drosophila* Models. *Frontiers in Cell and Developmental Biology*.
370 2019;7(85).
- 371 13. Zanconato F, Cordenonsi M, Piccolo S. YAP/TAZ at the Roots of Cancer. *Cancer Cell*.
372 2016;29(6):783-803.
- 373 14. Zhang W, Nandakumar N, Shi Y, Manzano M, Smith A, Graham G, et al. Downstream of
374 mutant KRAS, the transcription regulator YAP is essential for neoplastic progression to
375 pancreatic ductal adenocarcinoma. *Sci Signal*. 2014;7(324):ra42.
- 376 15. Mao Y, Sun S, Irvine KD. Role and regulation of Yap in KrasG12D-induced lung cancer.
377 *Oncotarget*. 2017;8(67):110877-89.
- 378 16. Valanne S, Wang JH, Ramet M. The *Drosophila* Toll signaling pathway. *J Immunol*.
379 2011;186(2):649-56.

- 380 17. Andersen DS, Colombani J, Palmerini V, Chakrabandhu K, Boone E, Rothlisberger M, et
381 al. The Drosophila TNF receptor Grindelwald couples loss of cell polarity and neoplastic growth.
382 Nature. 2015;522(7557):482-6.
- 383 18. Calleja M, Moreno E, Pelaz S, Morata G. Visualization of gene expression in living adult
384 Drosophila. Science. 1996;274(5285):252-5.
- 385 19. Birembaut P, Caron Y, Adnet JJ, Foidart JM. Usefulness of basement membrane markers
386 in tumoural pathology. J Pathol. 1985;145(4):283-96.
- 387 20. Ito K, Awano W, Suzuki K, Hiromi Y, Yamamoto D. The Drosophila mushroom body is
388 a quadruple structure of clonal units each of which contains a virtually identical set of neurones
389 and glial cells. Development. 1997;124(4):761-71.
- 390 21. Kango-Singh M, Singh A, Henry Sun Y. Eyeless collaborates with Hedgehog and
391 Decapentaplegic signaling in Drosophila eye induction. Dev Biol. 2003;256(1):49-60.
- 392 22. Dahmann C, Basler K. Opposing transcriptional outputs of Hedgehog signaling and
393 engrailed control compartmental cell sorting at the Drosophila A/P boundary. Cell.
394 2000;100(4):411-22.
- 395 23. Cellurale C, Sabio G, Kennedy NJ, Das M, Barlow M, Sandy P, et al. Requirement of c-
396 Jun NH(2)-terminal kinase for Ras-initiated tumor formation. Mol Cell Biol. 2011;31(7):1565-
397 76.
- 398 24. Uhlirova M, Jasper H, Bohmann D. Non-cell-autonomous induction of tissue overgrowth
399 by JNK/Ras cooperation in a Drosophila tumor model. Proc Natl Acad Sci U S A.
400 2005;102(37):13123-8.
- 401 25. Igaki T, Pagliarini RA, Xu T. Loss of cell polarity drives tumor growth and invasion
402 through JNK activation in Drosophila. Curr Biol. 2006;16(11):1139-46.
- 403 26. Martin-Blanco E, Gampel A, Ring J, Virdee K, Kirov N, Tolkovsky AM, et al. puckered
404 encodes a phosphatase that mediates a feedback loop regulating JNK activity during dorsal
405 closure in Drosophila. Genes Dev. 1998;12(4):557-70.
- 406 27. Uhlirova M, Bohmann D. JNK- and Fos-regulated Mmp1 expression cooperates with Ras
407 to induce invasive tumors in Drosophila. EMBO J. 2006;25(22):5294-304.
- 408 28. Deryugina EI, Quigley JP. Matrix metalloproteinases and tumor metastasis. Cancer
409 Metastasis Rev. 2006;25(1):9-34.
- 410 29. Beaucher M, Hersperger E, Page-McCaw A, Shearn A. Metastatic ability of Drosophila
411 tumors depends on MMP activity. Dev Biol. 2007;303(2):625-34.
- 412 30. Page-McCaw A, Serano J, Sante JM, Rubin GM. Drosophila matrix metalloproteinases
413 are required for tissue remodeling, but not embryonic development. Dev Cell. 2003;4(1):95-106.
- 414 31. Kauppila S, Maaty WS, Chen P, Tomar RS, Eby MT, Chapo J, et al. Eiger and its
415 receptor, Wengen, comprise a TNF-like system in Drosophila. Oncogene. 2003;22(31):4860-7.
- 416 32. Kanda H, Igaki T, Kanuka H, Yagi T, Miura M. Wengen, a member of the Drosophila
417 tumor necrosis factor receptor superfamily, is required for Eiger signaling. J Biol Chem.
418 2002;277(32):28372-5.

- 419 33. Muzzopappa M, Murcia L, Milan M. Feedback amplification loop drives malignant
420 growth in epithelial tissues. *Proc Natl Acad Sci U S A*. 2017;114(35):E7291-E300.
- 421 34. Willsey HR, Zheng X, Carlos Pastor-Pareja J, Willsey AJ, Beachy PA, Xu T. Localized
422 JNK signaling regulates organ size during development. *Elife*. 2016;5.
- 423 35. Atkins M, Potier D, Romanelli L, Jacobs J, Mach J, Hamaratoglu F, et al. An Ectopic
424 Network of Transcription Factors Regulated by Hippo Signaling Drives Growth and Invasion of
425 a Malignant Tumor Model. *Curr Biol*. 2016;26(16):2101-13.
- 426 36. Enomoto M, Kizawa D, Ohsawa S, Igaki T. JNK signaling is converted from anti- to pro-
427 tumor pathway by Ras-mediated switch of Warts activity. *Dev Biol*. 2015;403(2):162-71.
- 428 37. Liu B, Zheng Y, Yin F, Yu J, Silverman N, Pan D. Toll Receptor-Mediated Hippo
429 Signaling Controls Innate Immunity in *Drosophila*. *Cell*. 2016;164(3):406-19.
- 430 38. Hay BA, Wolff T, Rubin GM. Expression of baculovirus P35 prevents cell death in
431 *Drosophila*. *Development*. 1994;120(8):2121-9.
- 432 39. Goulev Y, Fauny JD, Gonzalez-Marti B, Flagiello D, Silber J, Zider A. SCALLOPED
433 interacts with YORKIE, the nuclear effector of the hippo tumor-suppressor pathway in
434 *Drosophila*. *Curr Biol*. 2008;18(6):435-41.
- 435 40. Wu S, Liu Y, Zheng Y, Dong J, Pan D. The TEAD/TEF family protein Scalloped
436 mediates transcriptional output of the Hippo growth-regulatory pathway. *Dev Cell*.
437 2008;14(3):388-98.
- 438 41. Zhang L, Ren F, Zhang Q, Chen Y, Wang B, Jiang J. The TEAD/TEF family of
439 transcription factor Scalloped mediates Hippo signaling in organ size control. *Dev Cell*.
440 2008;14(3):377-87.
- 441 42. Verghese S, Waghmare I, Kwon H, Hanes K, Kango-Singh M. Scribble acts in the
442 *Drosophila* fat-hippo pathway to regulate warts activity. *PLoS One*. 2012;7(11):e47173.
- 443 43. Rajalingam K, Schreck R, Rapp UR, Albert S. Ras oncogenes and their downstream
444 targets. *Biochim Biophys Acta*. 2007;1773(8):1177-95.
- 445 44. Liu AM, Xu Z, Luk JM. An update on targeting Hippo-YAP signaling in liver cancer.
446 *Expert Opin Ther Targets*. 2012;16(3):243-7.
- 447 45. Tournier C. The 2 Faces of JNK Signaling in Cancer. *Genes Cancer*. 2013;4(9-10):397-
448 400.
- 449 46. Sun G, Irvine KD. Regulation of Hippo signaling by Jun kinase signaling during
450 compensatory cell proliferation and regeneration, and in neoplastic tumors. *Dev Biol*.
451 2011;350(1):139-51.
- 452 47. Sun G, Irvine KD. Ajuba family proteins link JNK to Hippo signaling. *Sci Signal*.
453 2013;6(292):ra81.
- 454 48. Chen CL, Schroeder MC, Kango-Singh M, Tao C, Halder G. Tumor suppression by cell
455 competition through regulation of the Hippo pathway. *Proc Natl Acad Sci U S A*.
456 2012;109(2):484-9.

- 457 49. Doggett K, Grusche FA, Richardson HE, Brumby AM. Loss of the *Drosophila* cell
458 polarity regulator Scribbled promotes epithelial tissue overgrowth and cooperation with
459 oncogenic Ras-Raf through impaired Hippo pathway signaling. *BMC Dev Biol.* 2011;11:57.
- 460 50. Bunker BD, Nellimoottil TT, Boileau RM, Classen AK, Bilder D. The transcriptional
461 response to tumorigenic polarity loss in *Drosophila*. *Elife.* 2015;4.
- 462 51. Zanconato F, Forcato M, Battilana G, Azzolin L, Quaranta E, Bodega B, et al. Genome-
463 wide association between YAP/TAZ/TEAD and AP-1 at enhancers drives oncogenic growth. *Nat*
464 *Cell Biol.* 2015;17(9):1218-27.
- 465 52. Patel PH, Dutta D, Edgar BA. Niche appropriation by *Drosophila* intestinal stem cell
466 tumours. *Nat Cell Biol.* 2015;17(9):1182-92.
- 467 53. Kulshammer E, Mundorf J, Kilinc M, Frommolt P, Wagle P, Uhlirova M. Interplay
468 among *Drosophila* transcription factors Ets21c, Fos and Ftz-F1 drives JNK-mediated tumor
469 malignancy. *Dis Model Mech.* 2015;8(10):1279-93.
- 470 54. Oh H, Reddy BV, Irvine KD. Phosphorylation-independent repression of Yorkie in Fat-
471 Hippo signaling. *Dev Biol.* 2009;335(1):188-97.
- 472 55. Morimoto K, Tamori Y. Induction and Diagnosis of Tumors in *Drosophila* Imaginal Disc
473 Epithelia. *J Vis Exp.* 2017(125).
- 474 56. Cong B, Ohsawa S, Igaki T. JNK and Yorkie drive tumor progression by generating
475 polyploid giant cells in *Drosophila*. *Oncogene.* 2018;37(23):3088-97.
- 476 57. Bell CD, Waizbard E. Variability of cell size in primary and metastatic human breast
477 carcinoma. *Invasion Metastasis.* 1986;6(1):11-20.
- 478 58. Ma X, Chen Y, Xu W, Wu N, Li M, Cao Y, et al. Impaired Hippo signaling promotes
479 Rho1-JNK-dependent growth. *Proc Natl Acad Sci U S A.* 2015;112(4):1065-70.
- 480 59. Yu FX, Zhao B, Panupinthu N, Jewell JL, Lian I, Wang LH, et al. Regulation of the
481 Hippo-YAP pathway by G-protein-coupled receptor signaling. *Cell.* 2012;150(4):780-91.
- 482 60. Ramet M, Lanot R, Zachary D, Manfruelli P. JNK signaling pathway is required for
483 efficient wound healing in *Drosophila*. *Dev Biol.* 2002;241(1):145-56.
- 484 61. Page-McCaw A, Ewald AJ, Werb Z. Matrix metalloproteinases and the regulation of
485 tissue remodelling. *Nat Rev Mol Cell Biol.* 2007;8(3):221-33.
- 486 62. Baldwin AS, Jr. The NF-kappa B and I kappa B proteins: new discoveries and insights.
487 *Annu Rev Immunol.* 1996;14:649-83.
- 488 63. Xia Y, Shen S, Verma IM. NF-kappaB, an active player in human cancers. *Cancer*
489 *Immunol Res.* 2014;2(9):823-30.
- 490 64. Wu C, Chen C, Dai J, Zhang F, Chen Y, Li W, et al. Toll pathway modulates TNF-
491 induced JNK-dependent cell death in *Drosophila*. *Open Biol.* 2015;5(7):140171.
- 492 65. Zhang JY, Tao S, Kimmel R, Khavari PA. CDK4 regulation by TNFR1 and JNK is
493 required for NF-kappaB-mediated epidermal growth control. *J Cell Biol.* 2005;168(4):561-6.

- 494 66. Maglic D, Schlegelmilch K, Dost AF, Panero R, Dill MT, Calogero RA, et al. YAP-
495 TEAD signaling promotes basal cell carcinoma development via a c-JUN/AP1 axis. *EMBO J.*
496 2018;37(17).
- 497 67. Nowell CS, Odermatt PD, Azzolin L, Hohnel S, Wagner EF, Fantner GE, et al. Chronic
498 inflammation imposes aberrant cell fate in regenerating epithelia through mechanotransduction.
499 *Nat Cell Biol.* 2016;18(2):168-80.
- 500 68. Taniguchi K, Wu LW, Grivennikov SI, de Jong PR, Lian I, Yu FX, et al. A gp130-Src-
501 YAP module links inflammation to epithelial regeneration. *Nature.* 2015;519(7541):57-62.
- 502 69. Kango-Singh M, Nolo R, Tao C, Verstrecken P, Hiesinger PR, Bellen HJ, et al. Shar-pei
503 mediates cell proliferation arrest during imaginal disc growth in *Drosophila*. *Development.*
504 2002;129(24):5719-30.

505

506

507 **Figure legends**

508 **Figure 1: Expression of Oncogenic Yki (Yki^{3SA}) in *scrib* mutant cells forms invasive tumors**

509 (A-A') Mature 3rd instar larvae from *nub>GFP* (A) and *nub>Yki^{3SA}scrib^{RNAi}* (A') show growth of
510 wing discs (GFP, grey). (B-B'') Panels show (B) rabbit anti-Laminin (red) expression in
511 *nub>Yki^{3SA}scrib^{RNAi}* (GFP, green) wing disc (60X magnification). The inset (B') shows discs
512 labelled by Laminin (red) to test motility of tumor cells (green). Panel (B'') shows the XZ and
513 YZ sections of the panel (B) highlighting the invasive cell (arrow). (C-F) Expression of *puc^{E69}*-
514 *lacz* tracked with mouse anti- β -gal antibody (red, grey) in (C) *Yki^{3SA}scrib^{RNAi}puc^{E69}* and (D)
515 *Ras^{V12}scrib^{RNAi}puc^{E69}* clones (green). Panels show expression of MMP1 labelled with mouse
516 anti-MMP1 antibody (red, grey) in (E) *Yki^{3SA}scrib^{RNAi}* and (F) *Ras^{V12}scrib^{RNAi}* clones (green). (G)
517 Graph shows quantification of MMP1 expression in *Yki^{3SA}scrib^{RNAi}* tumor (GFP expressing
518 clone) and normal cells (non-GFP expressing cells outside the clone). Paired student T test with
519 n=5, 95% confidence was performed using Graphpad Prism 5, p < 0.0001.

520

521 **Figure 1: Role of Cact in tumor progression**

522 Panels show Cact expression (red, grey) in GFP-labelled clones (Green) from (A) *AyGal4>GFP*,
523 (B) *AyGal4>scrib^{RNAi}*, (C) *AyGAL4>Yki^{3SA}* and, (D) *AyGAL4> Yki^{3SA}scrib^{RNAi}* wing discs. (F-I)
524 pJNK (red, grey) and (K-N) MMP1 expression (red, grey) in clones (green) when Cact is
525 downregulated. (E, J, O) Bar graphs depict quantification of change in Cact (E), pJNK (J) and
526 MMP1 (O) expression between indicated genotypes. *= p<0.05, ns= not significant

527

528 **Figure 2: Effect of downregulating both the TNF receptors on the Tumor progression**

529 Panels show wing imaginal discs containing heat-shock induced GFP labelled (green) clones
530 expressing *wgn^{RNAi}* in the indicated genotypes stained with Rb anti-pJNK antibody (**A-D**) or anti-
531 MMP1 antibody (**G-J**). (**E, J-L**) Bar graphs showing quantification of pJNK (**E, K**) and MMP1
532 (**F, L**) expression amongst indicated genotypes. *= p<0.05, ns= not significant

533

534 **Figure 4: JNK is the key regulator of tumor invasiveness**

535 Panels (**A-B'**, **E-F'**, **H-H'**) show GFP-labelled heat-shock clones (green) in the wing imaginal
536 discs of *Yki^{3SA}scrib^{RNAi}bsk^{DN}* (**A, E, H**) and *Yki^{3SA}scrib^{RNAi}bsk^{DN}wgn^{RNAi}* (**B, F**) stained for
537 antibodies against pJNK (red, grey) (**A, B**), MMP1 (red, grey) (**E, F**), and Cact (red, grey) (**H**).
538 (**C**) Thickness of the clones representing the multi-layered structure of indicated genotypes was
539 measured using Photoshop, n=8. (**D, G, I**) Bar graphs show quantification of change in
540 expression of pJNK (**D**), MMP1 (**G**) and Cact (**I**) amongst indicated genotype. *= p<0.05, ns=
541 not significant

542

543 **Figure 5: Role of Yki in stimulating Cact and promoting tumorigenesis**

544 Panels **A-F** show effect of downregulating *yki* (*UASyki^{RNAi}*) in the GFP-labelled heat-shock
545 clones (green) in wing imaginal discs from larvae of the indicated genotype. (**A-D**) Confocal
546 images present effect of *yki^{RNAi}* on Cact (red, grey) expression. (**E-G**) Graphs show quantification
547 of clone size (**E**), clone thickness (**F**), and change in Cact expression levels (**G**). Panels **H-L**
548 show effects of *sd* downregulation (*UASsd^{RNAi}*) on *nubGal4* driven tumor phenotypes in the wing
549 imaginal discs. (**H-K**) Confocal images of wing discs from indicated genotypes stained with anti-
550 Cact antibody (red, grey) are presented. (**L**) Graph showing quantification of changes in Cact
551 expression. *= p<0.05, ns= not significant

552

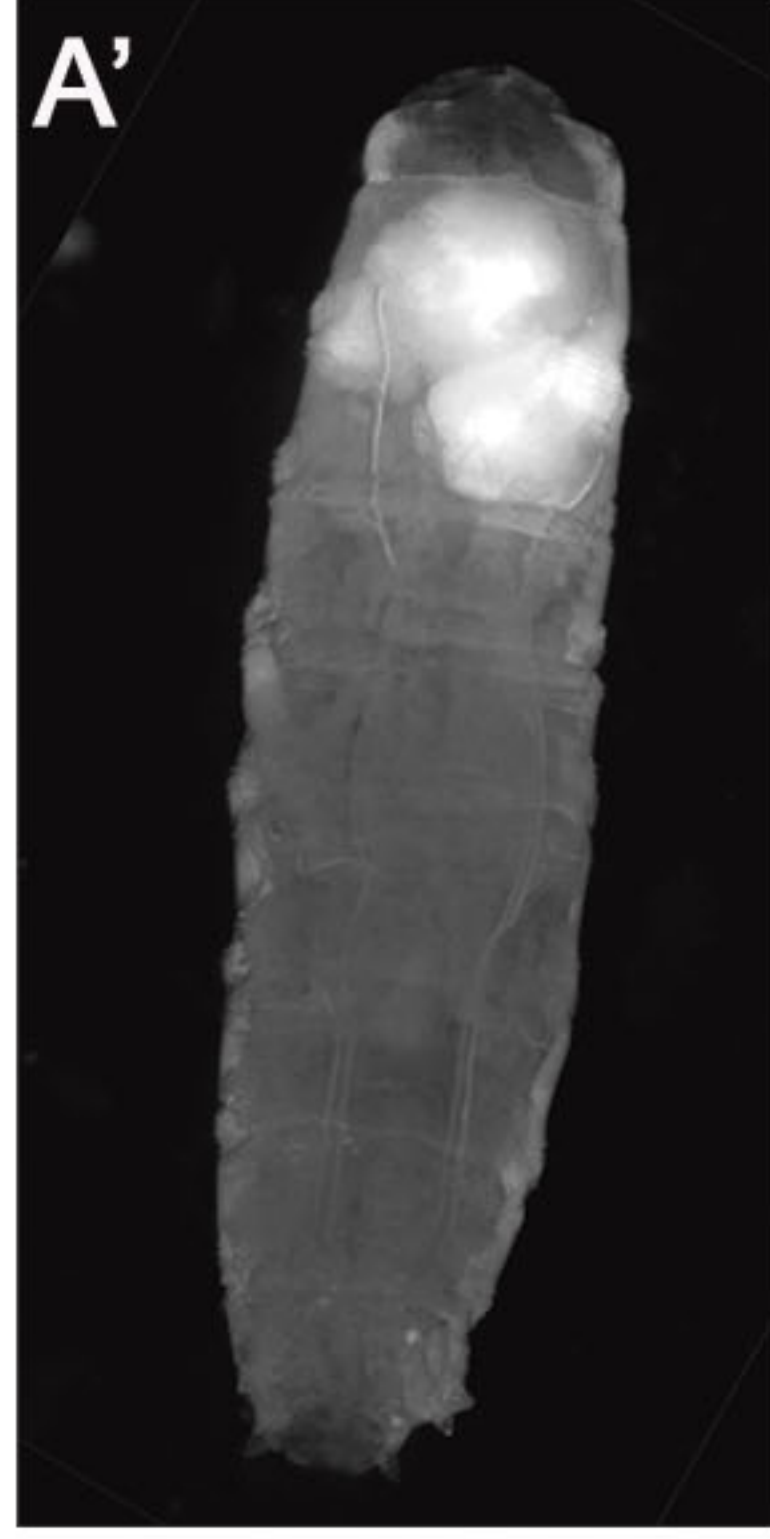
553 **Figure 6: Model for Yki mediated Cact and JNK activation promoting tumorigenesis**

554 A model depicting the downstream effects of the cooperation between activated oncogene (*Yki* or
555 *Ras*) and loss of polarity gene, *scrib* is shown. In somatic clones (elliptical cells), JNK is
556 activated by TNF pathway ligand Egr and its receptors, Wgn and Grnd. Independently, JNK can
557 be activated in the tumor cells due to Cact accumulation via Yki activation. Yki mediated Cact
558 and JNK activation is critical for tumor progression.

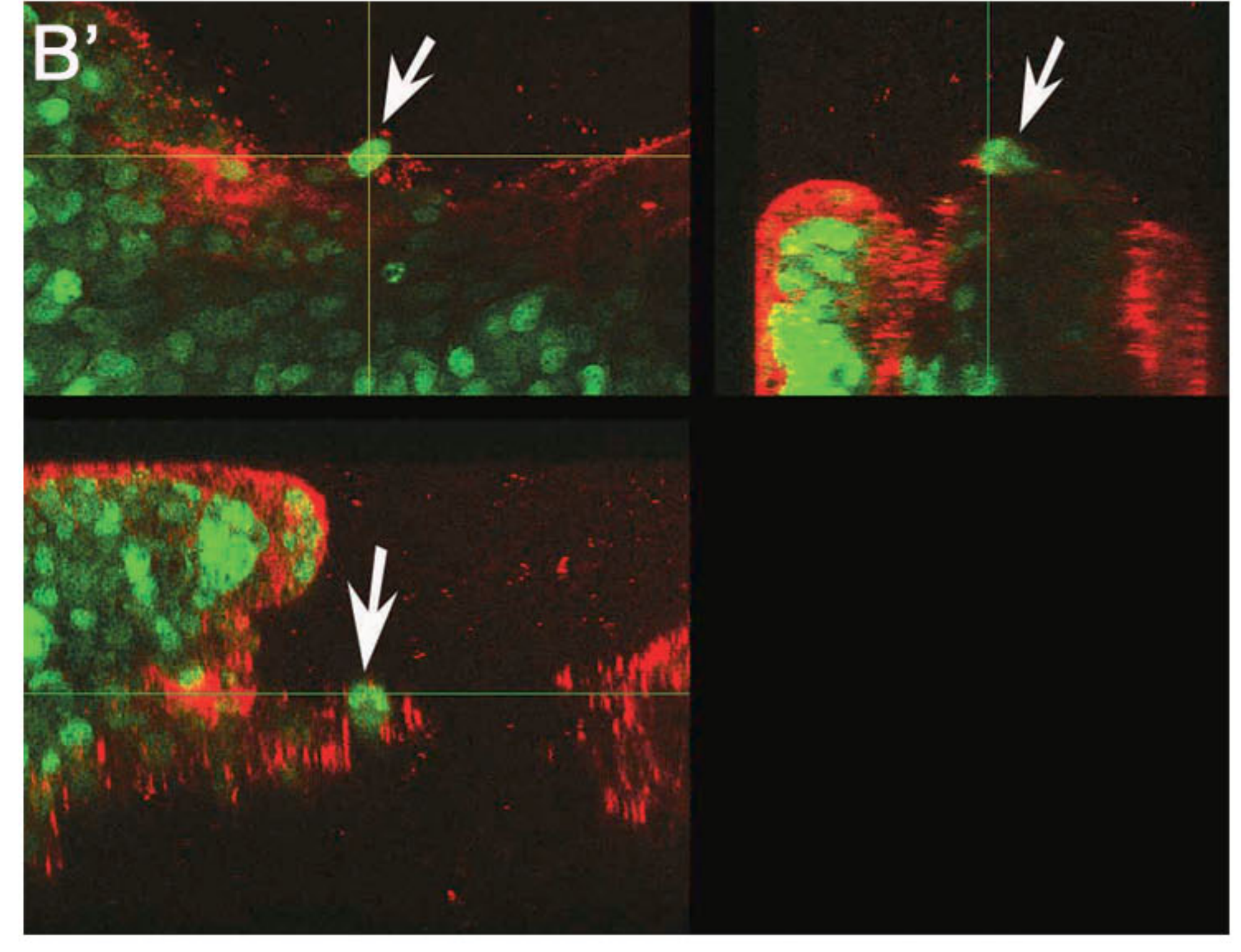
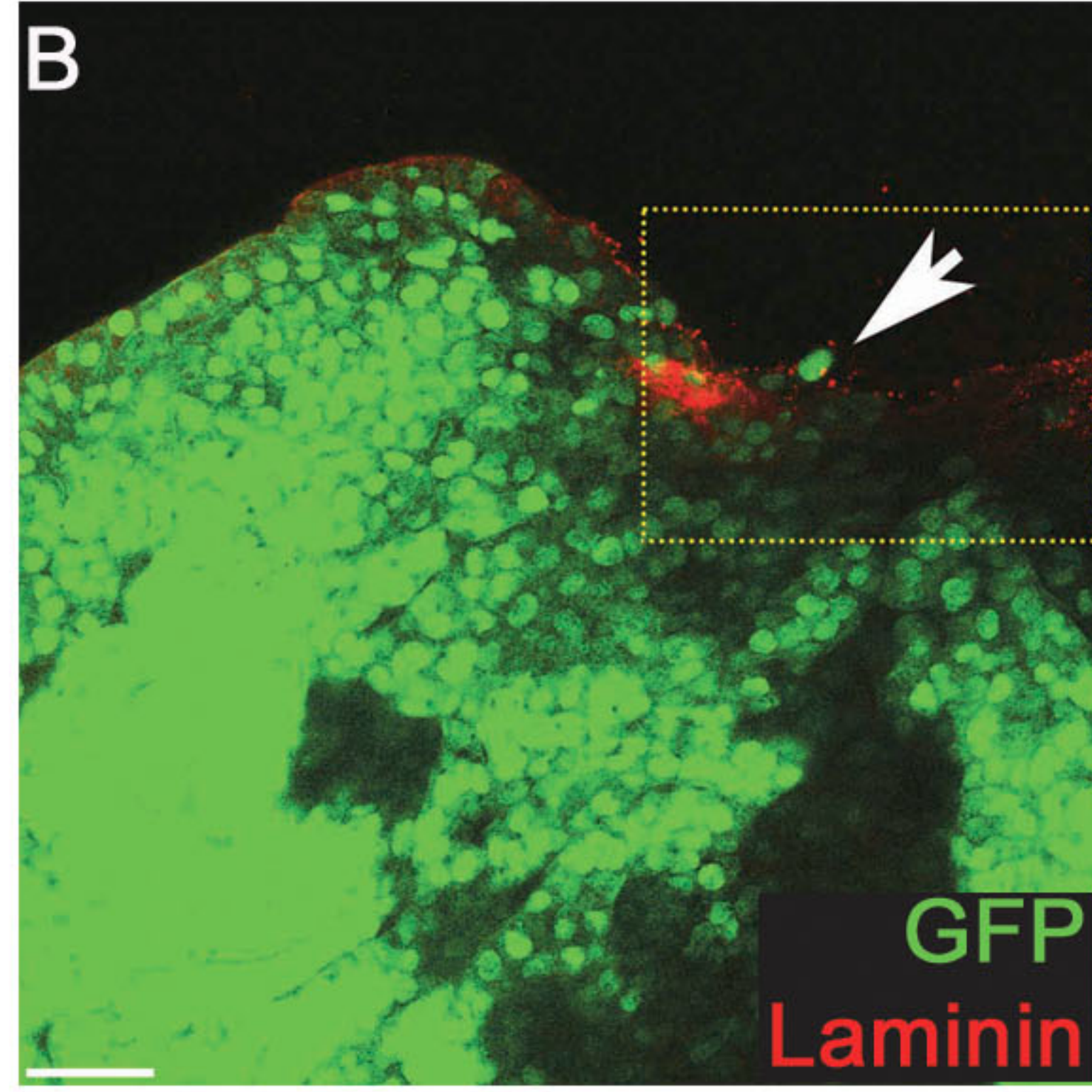
nubGAL4
UASGFP



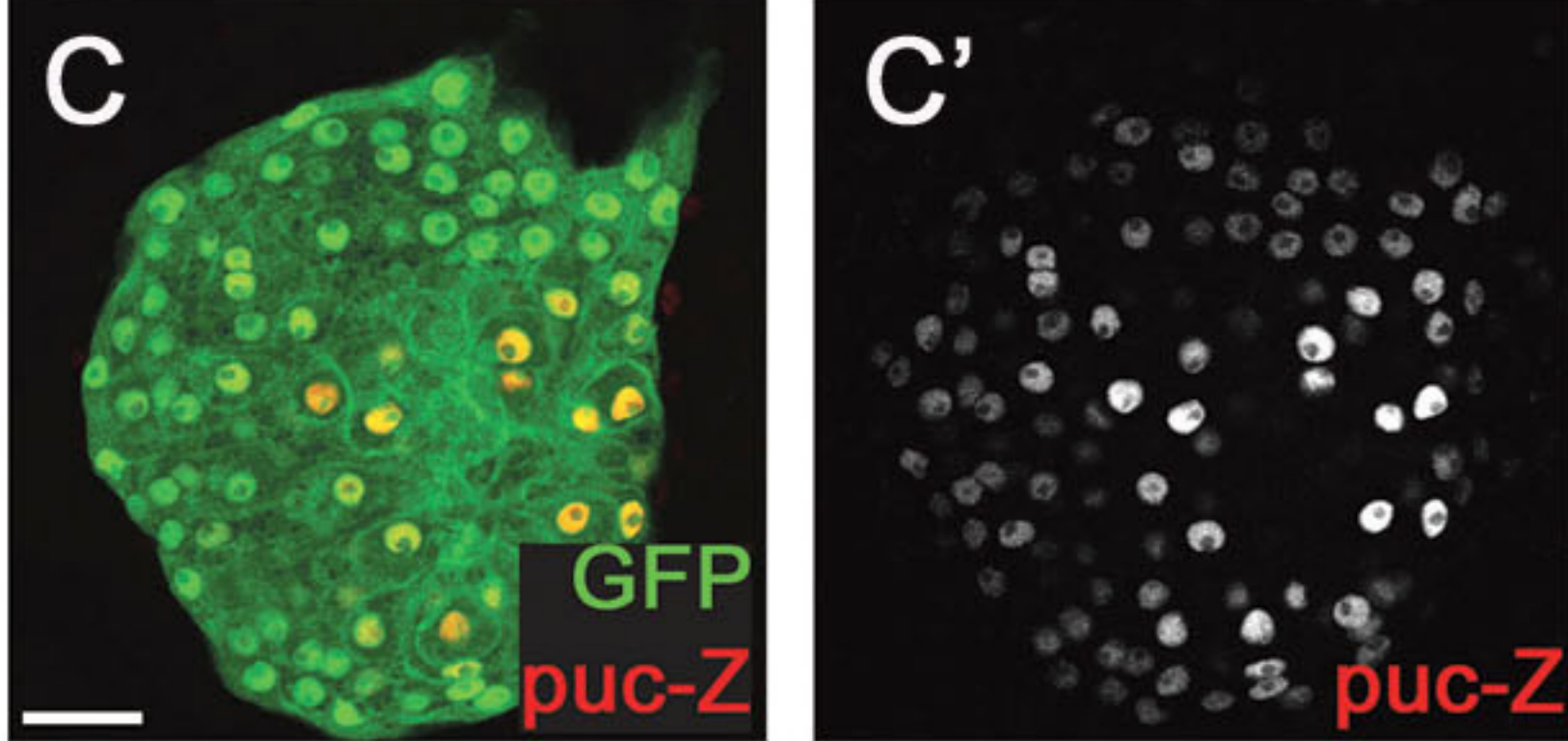
nubGFP UAS Yki^{3SA}
UAS scrib^{RNAi}



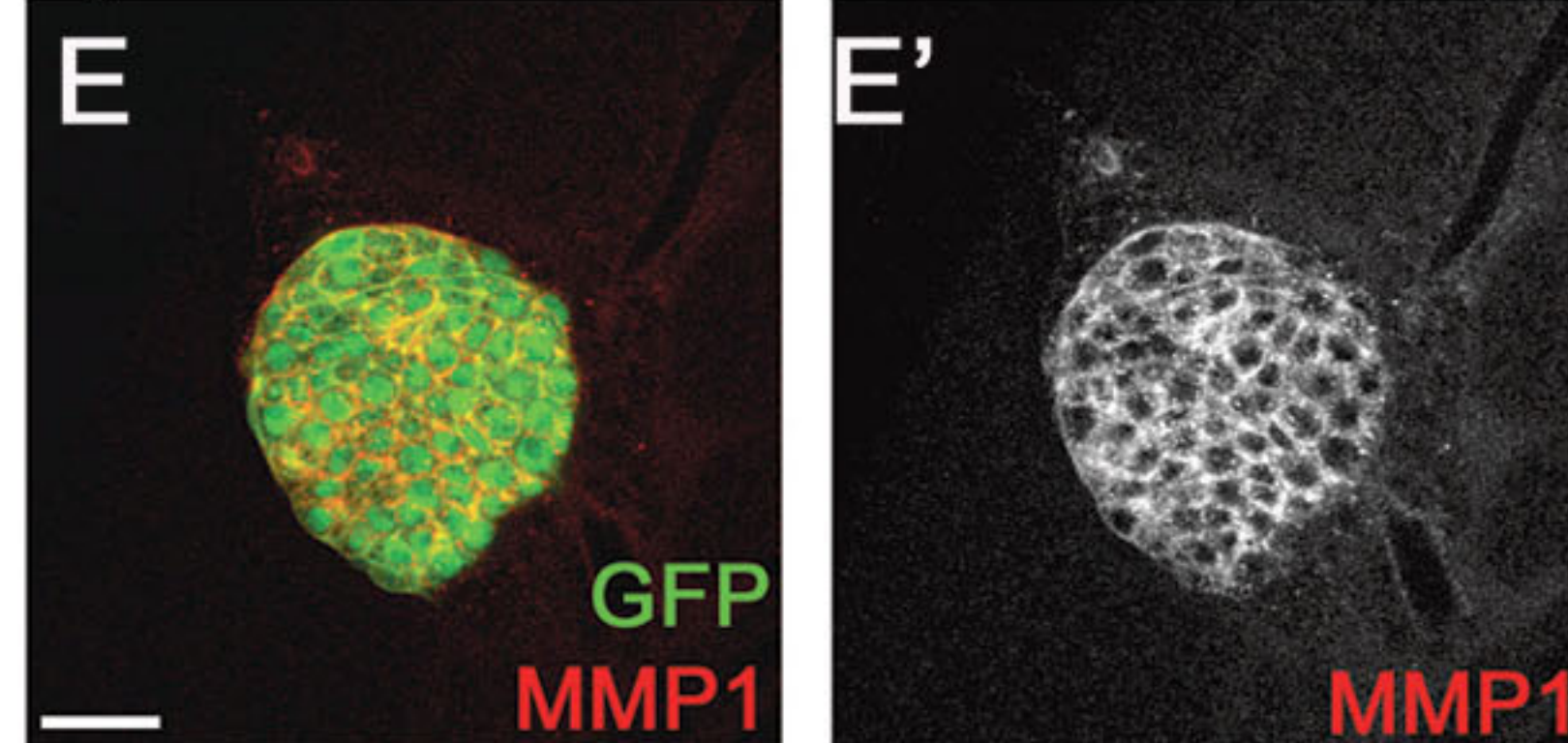
nubGFP UAS Yki^{3SA} UAS scrib^{RNAi}



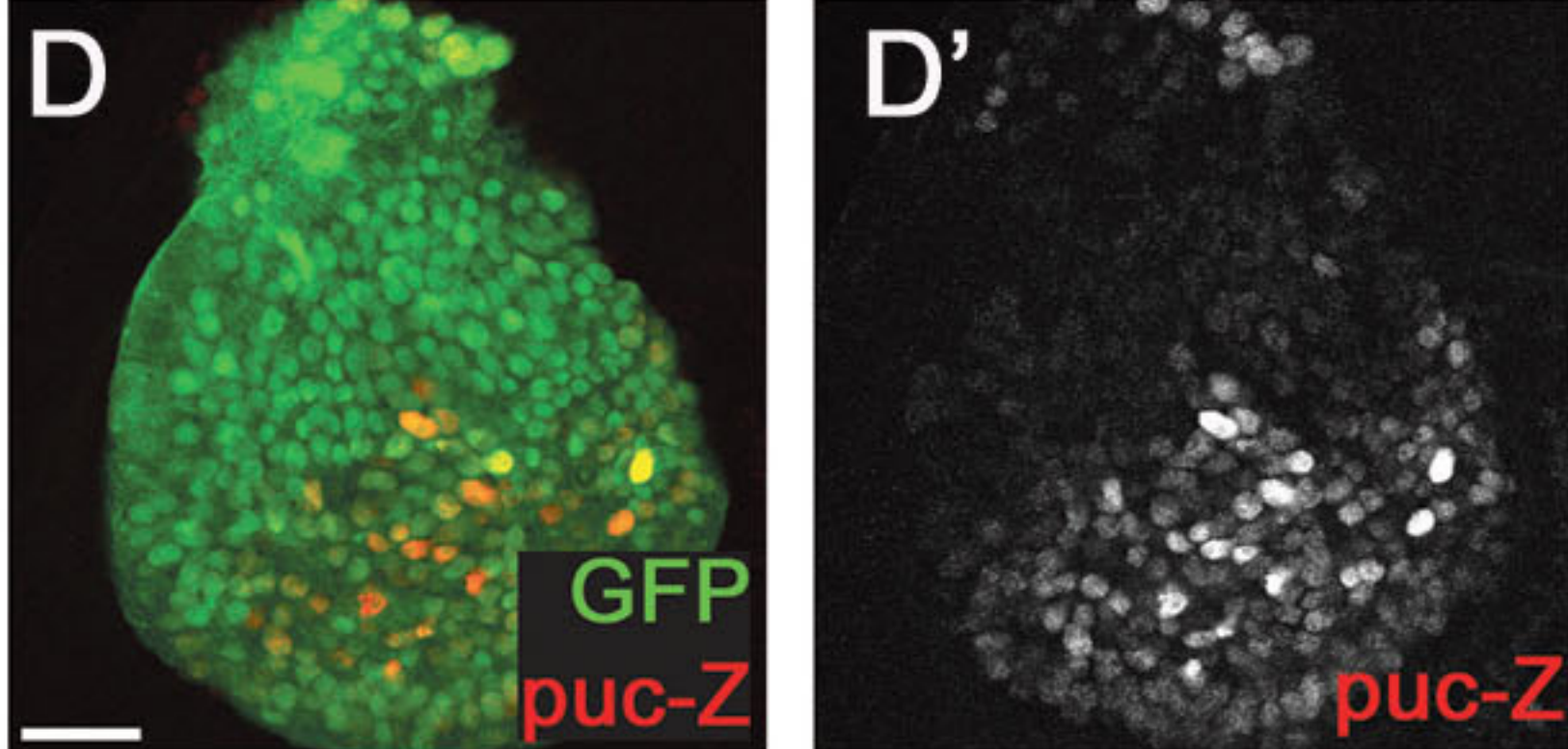
AyGFP UAS Yki^{3SA} UAS scrib^{RNAi}



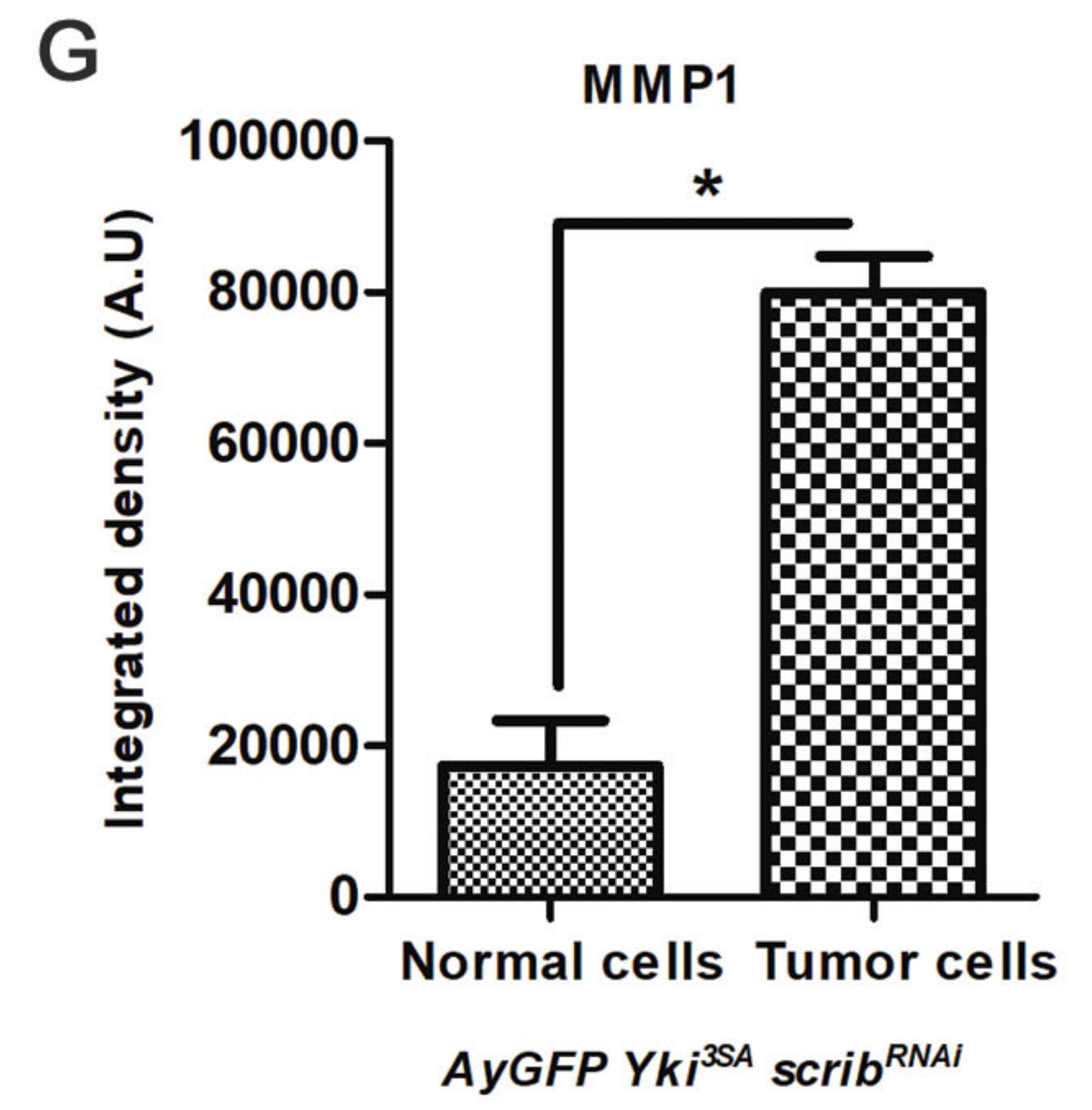
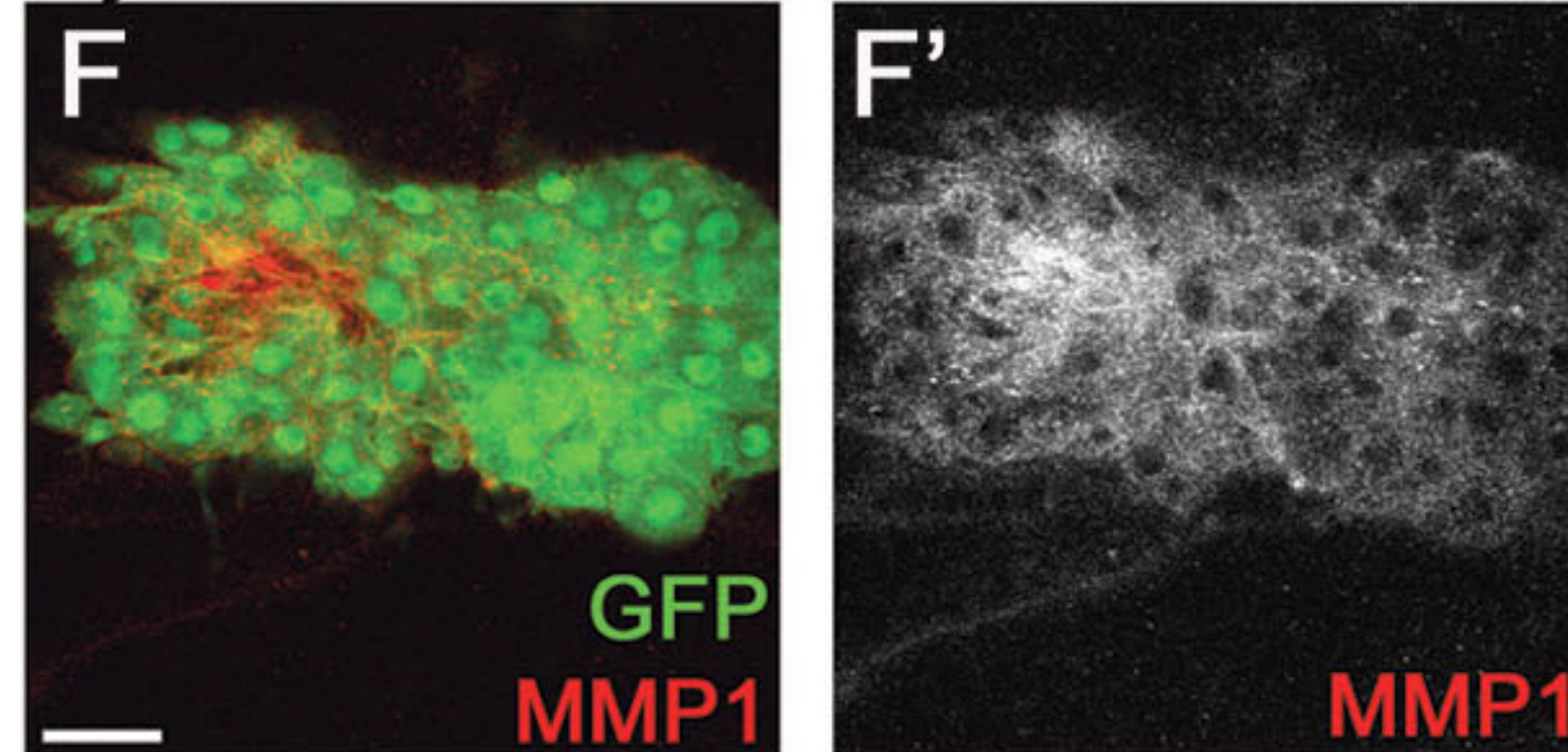
AyGFP UAS Yki^{3SA} UAS scrib^{RNAi}

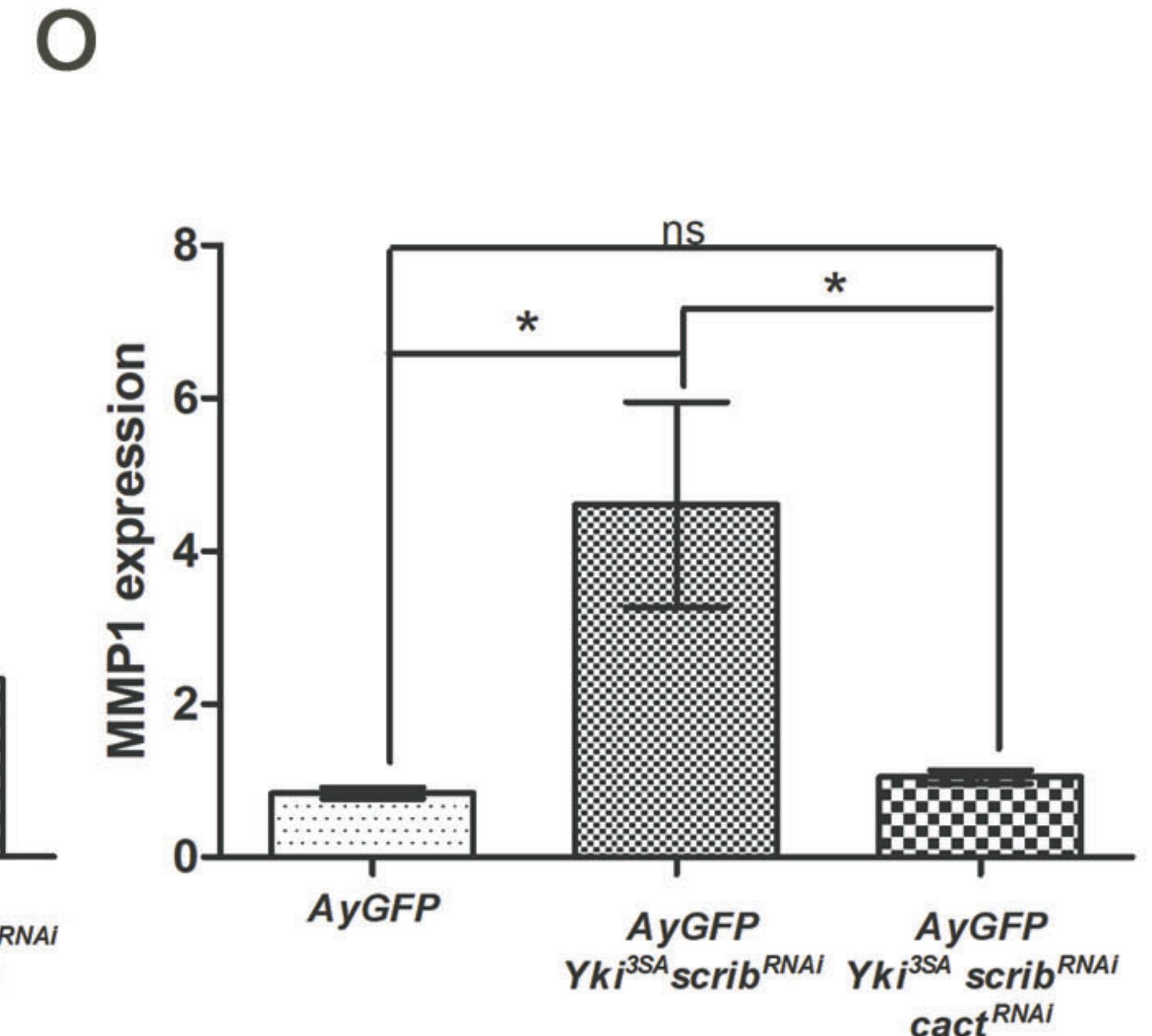
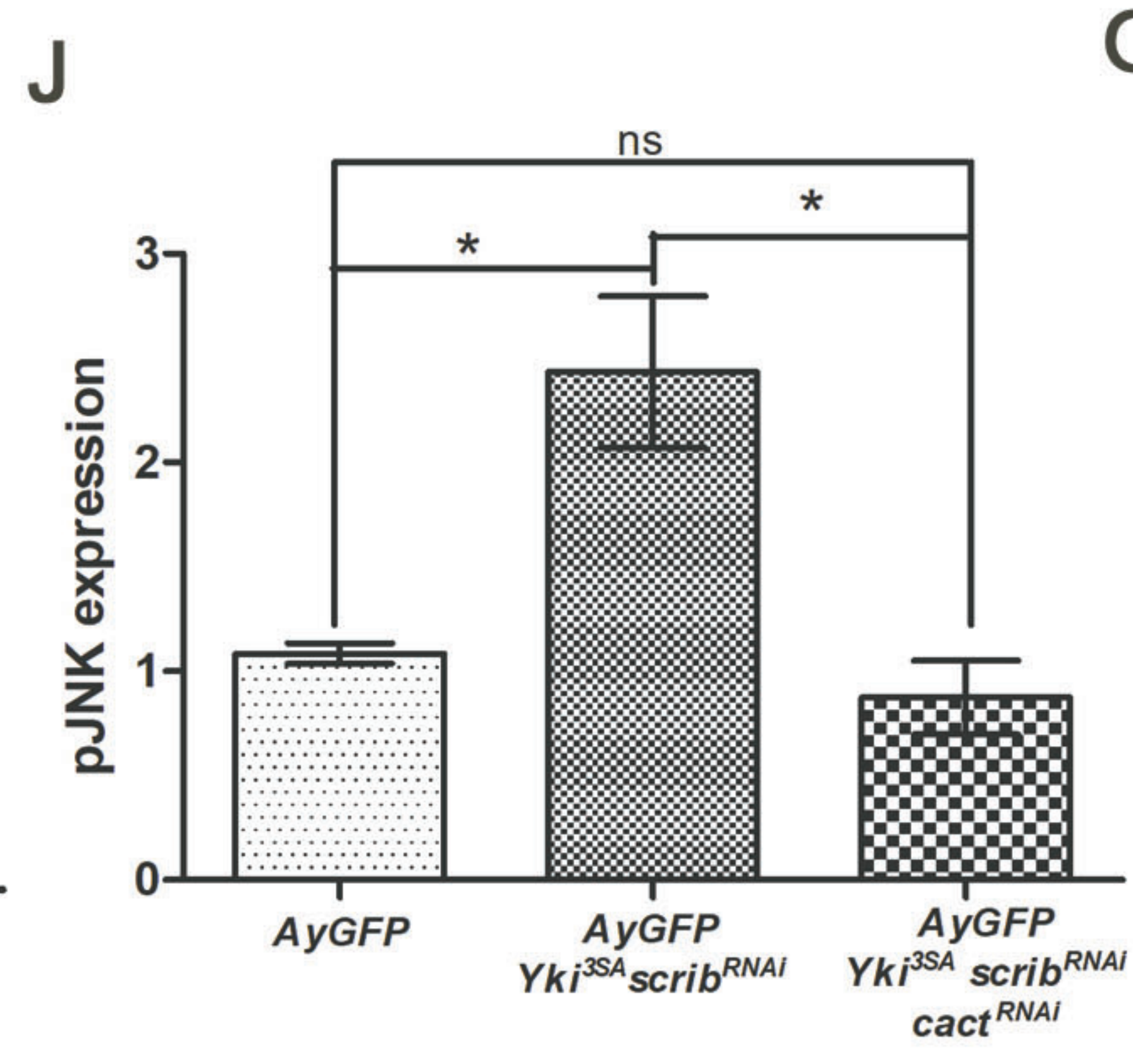
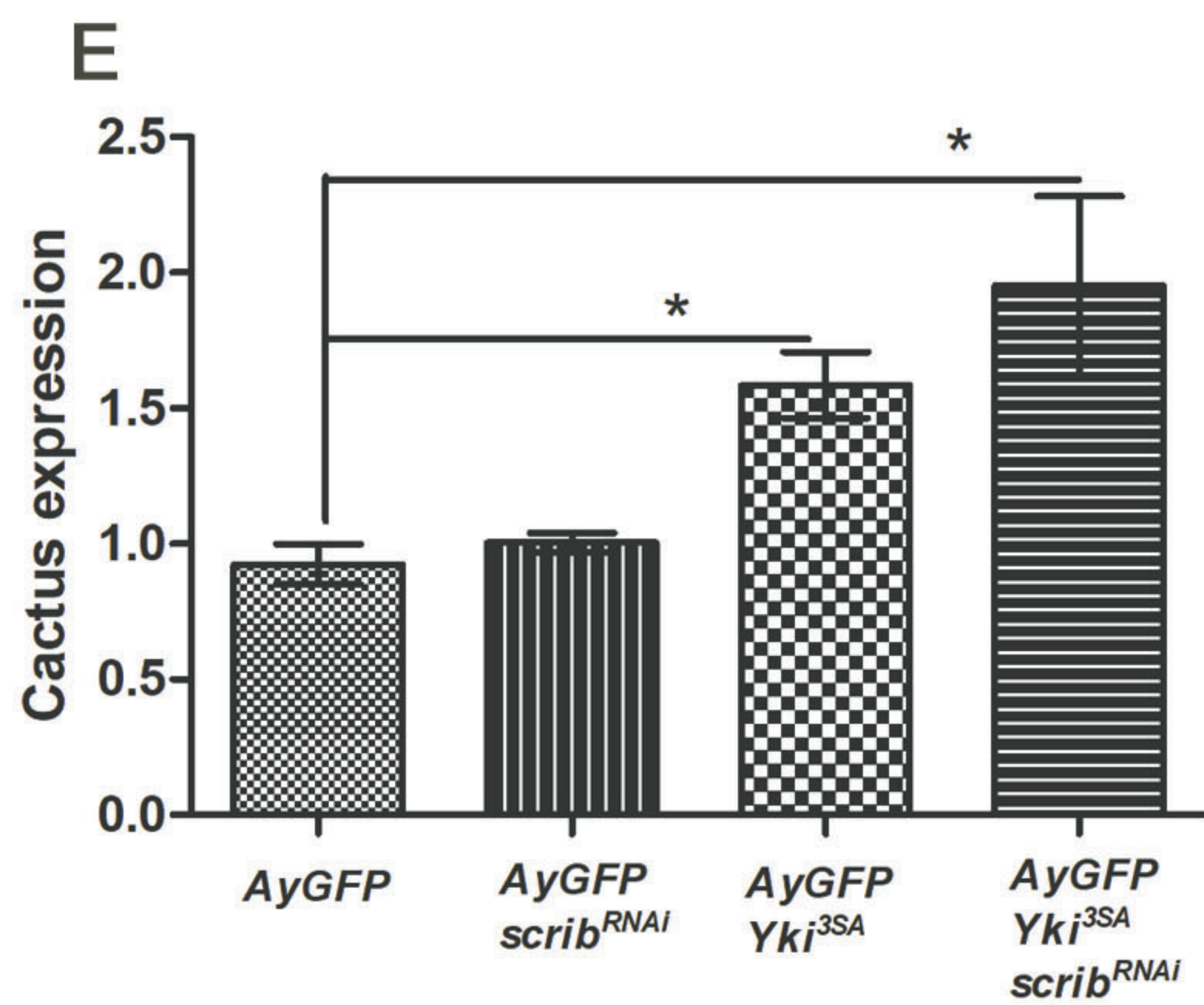
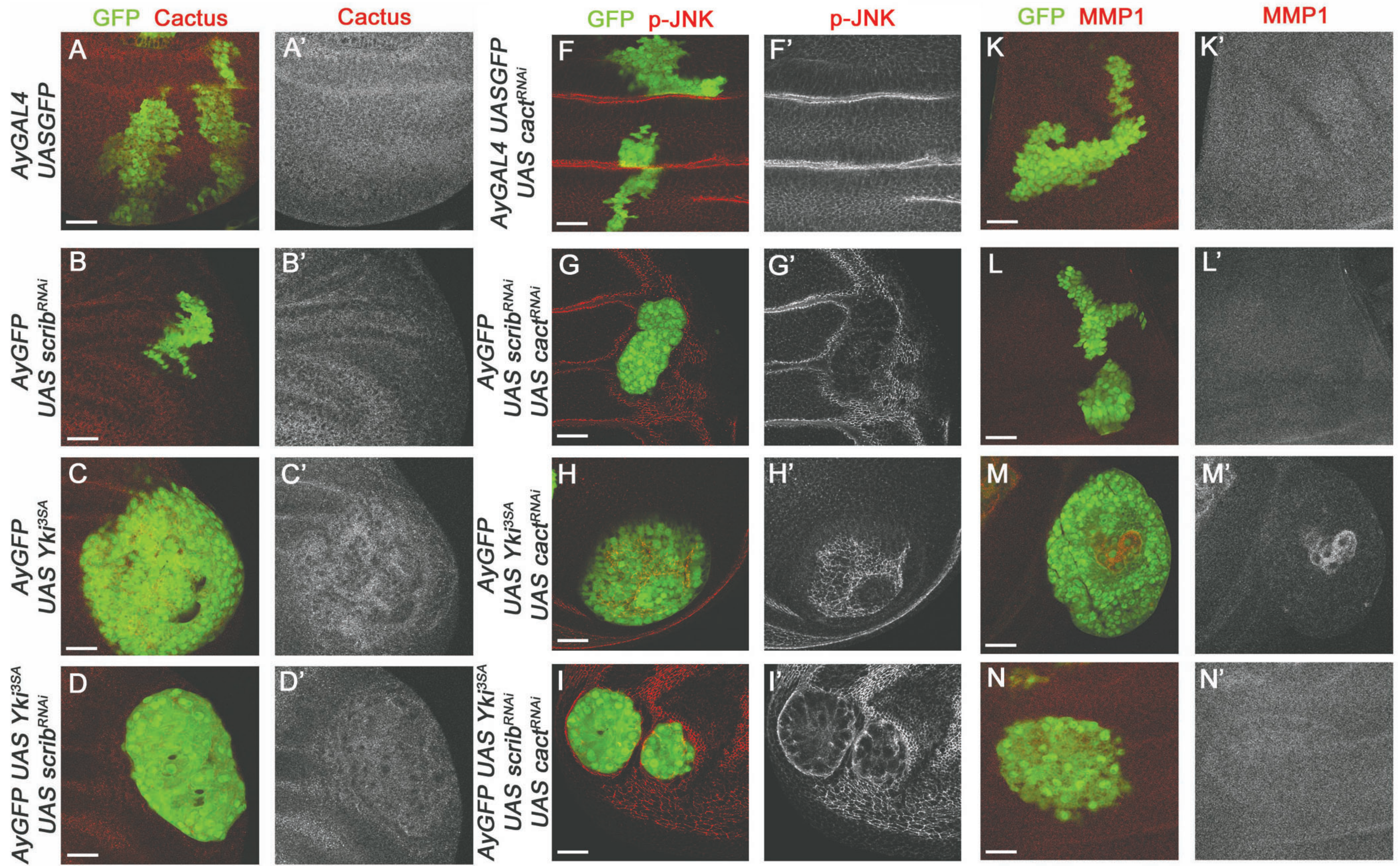


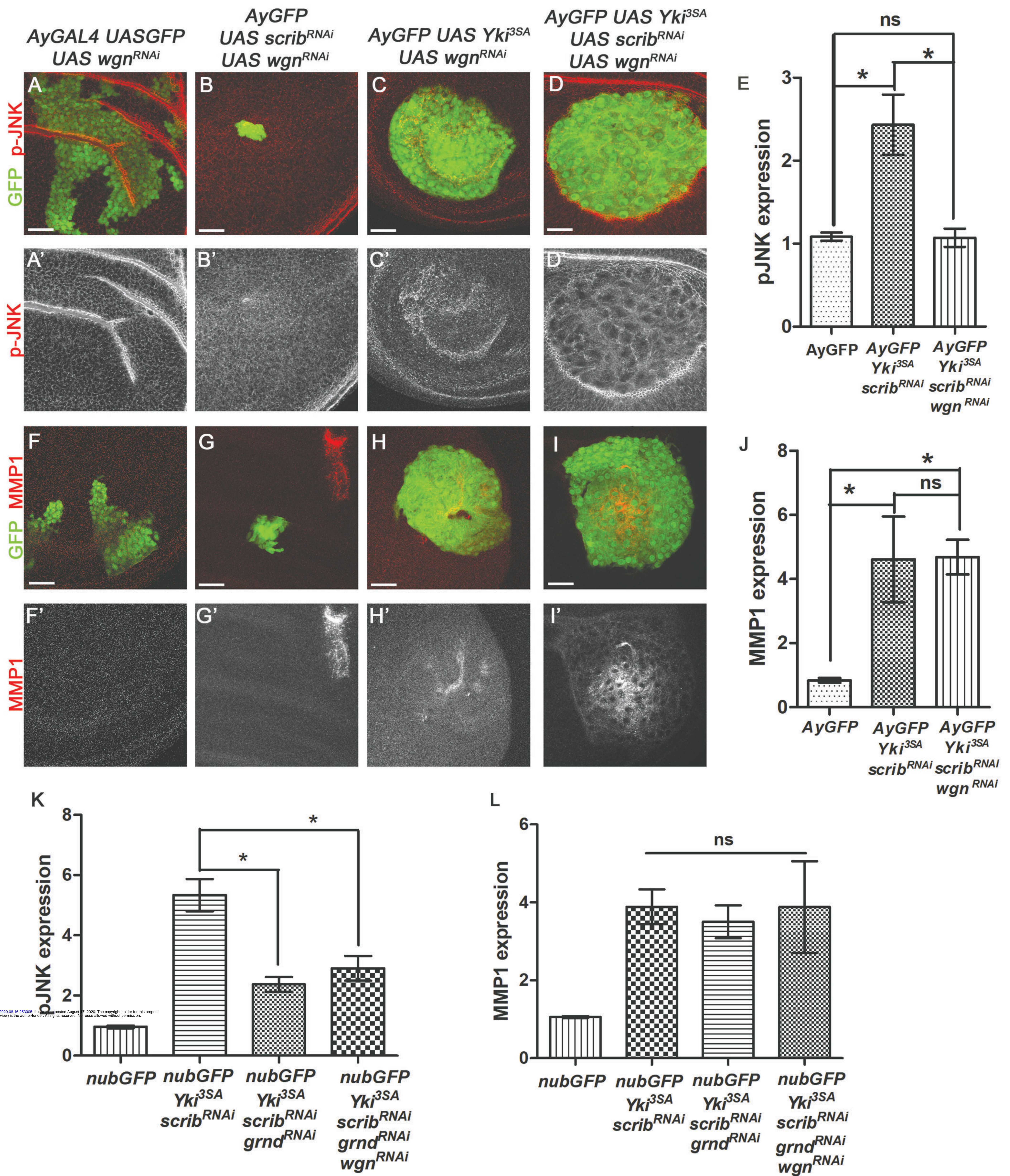
AyGFP UAS Ras^{V12} UAS scrib^{RNAi}



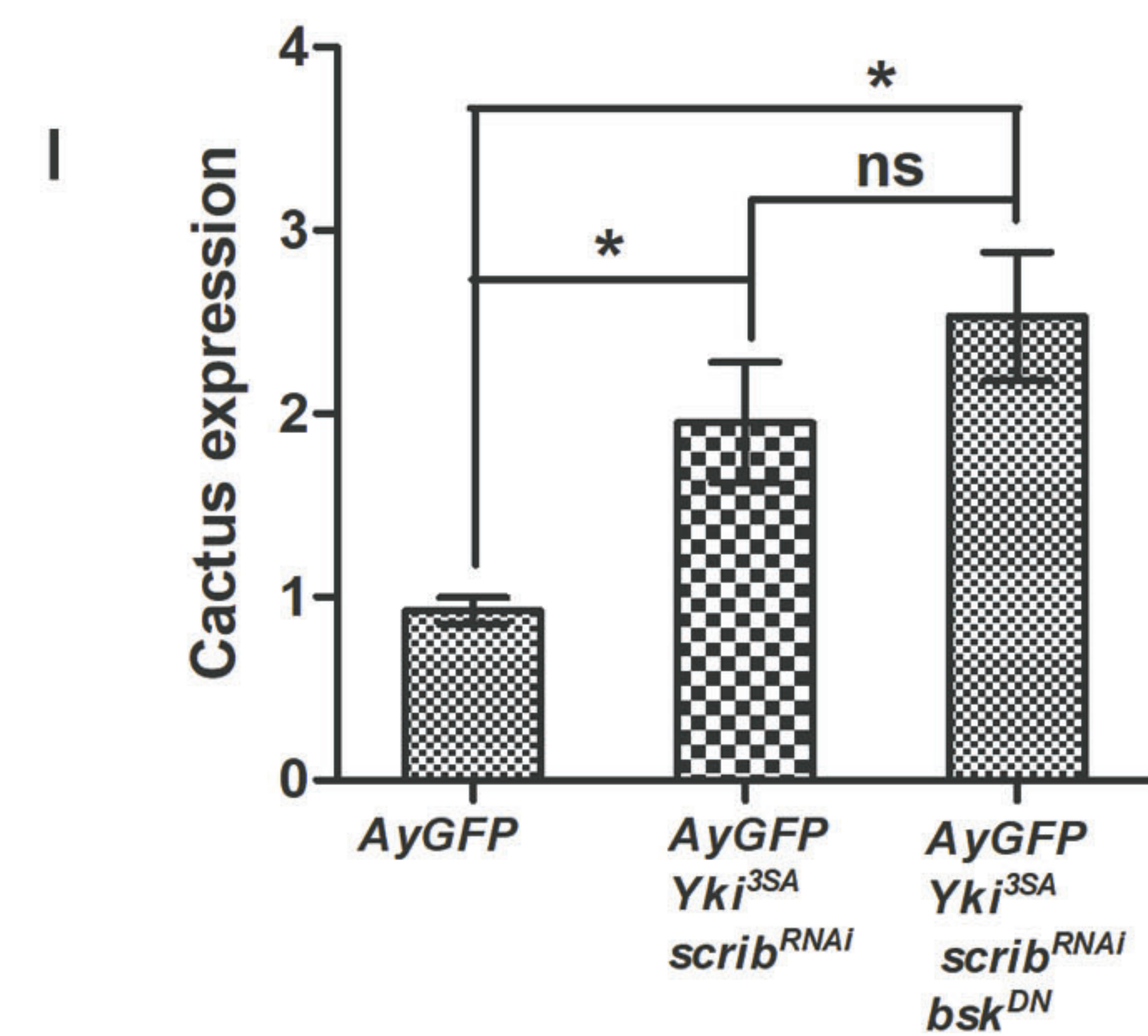
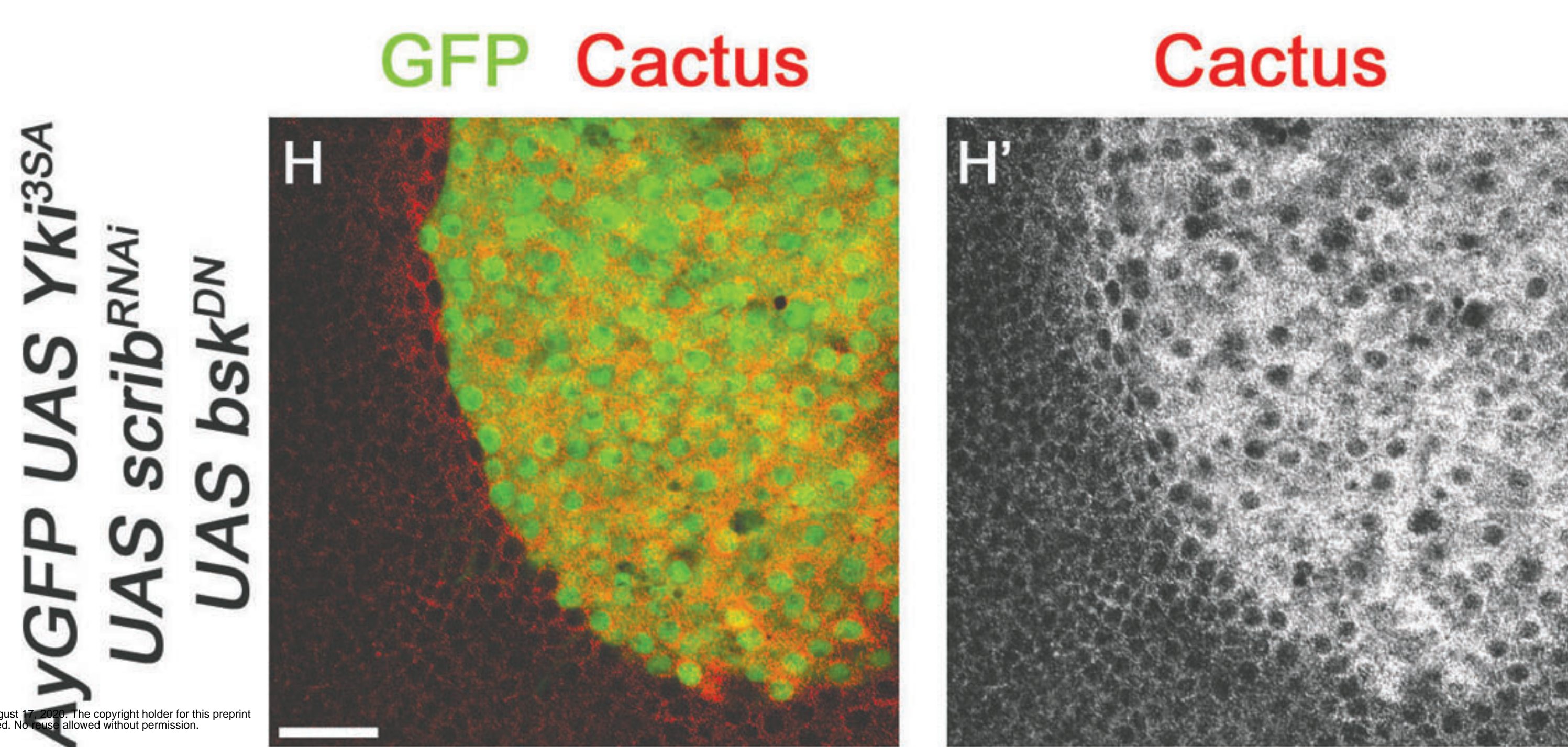
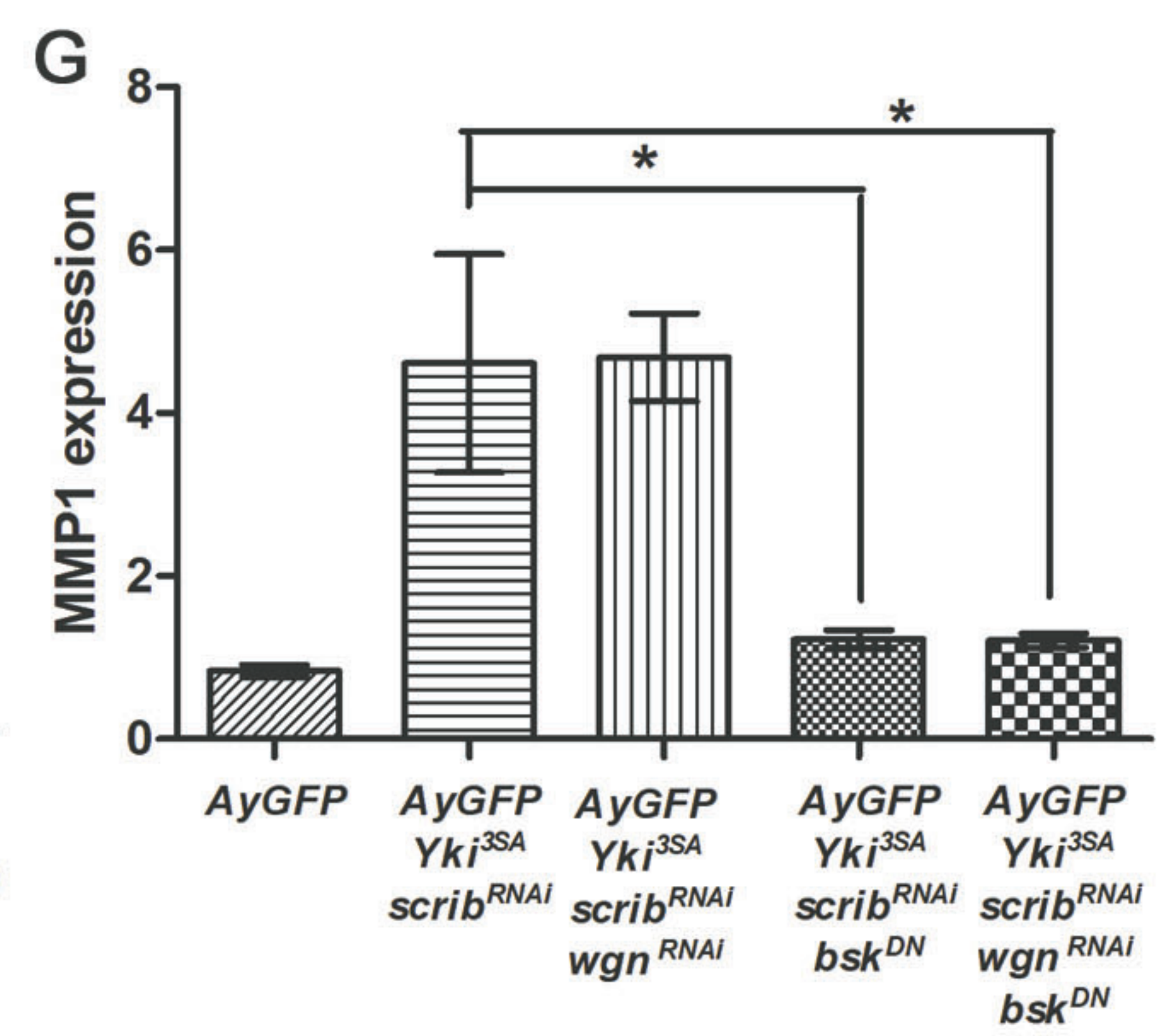
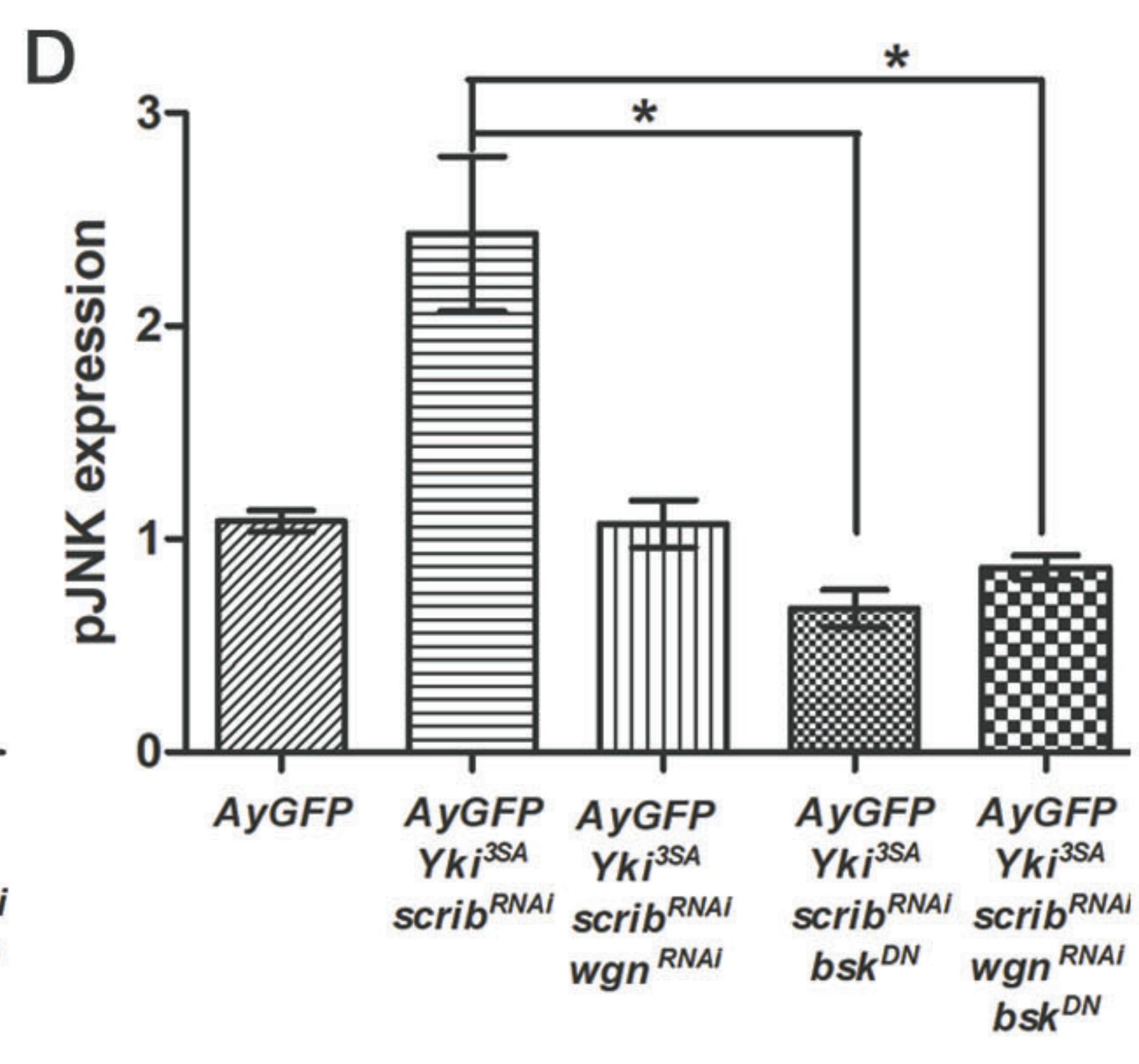
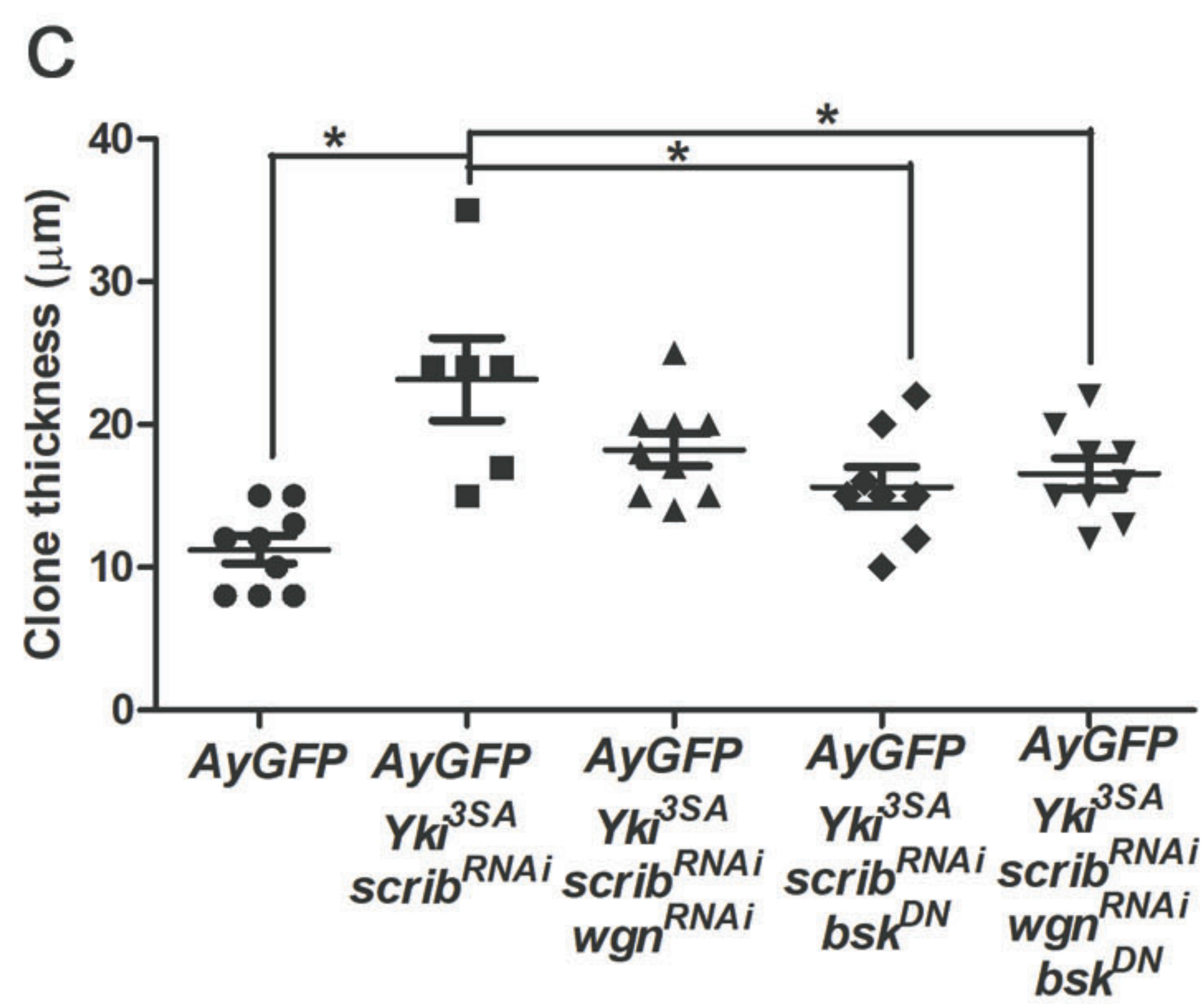
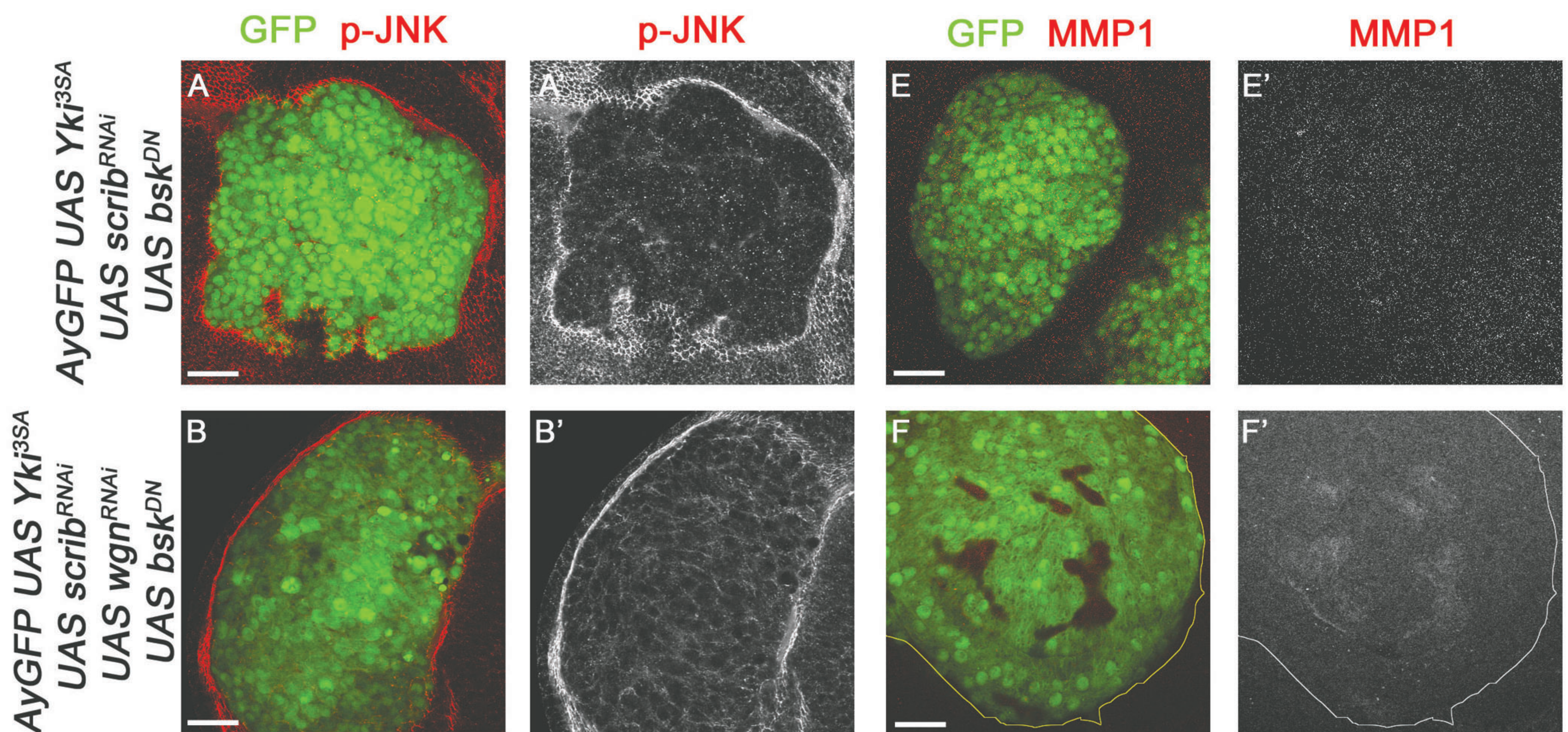
AyGFP UAS Ras^{V12} UAS scrib^{RNAi}







Snigha et al Figure 3



Snigdha et al., Figure 4

